

2024 European School on Magnetism

27 August - 6 September 2024, York, UK

Spin wave resonance techniques

Burkard Hillebrands

Fachbereich Physik and Landesforschungszentrum OPTIMAS
Rheinland-Pfälzische Technische Universität Kaiserslautern-Landau
Kaiserslautern, Germany

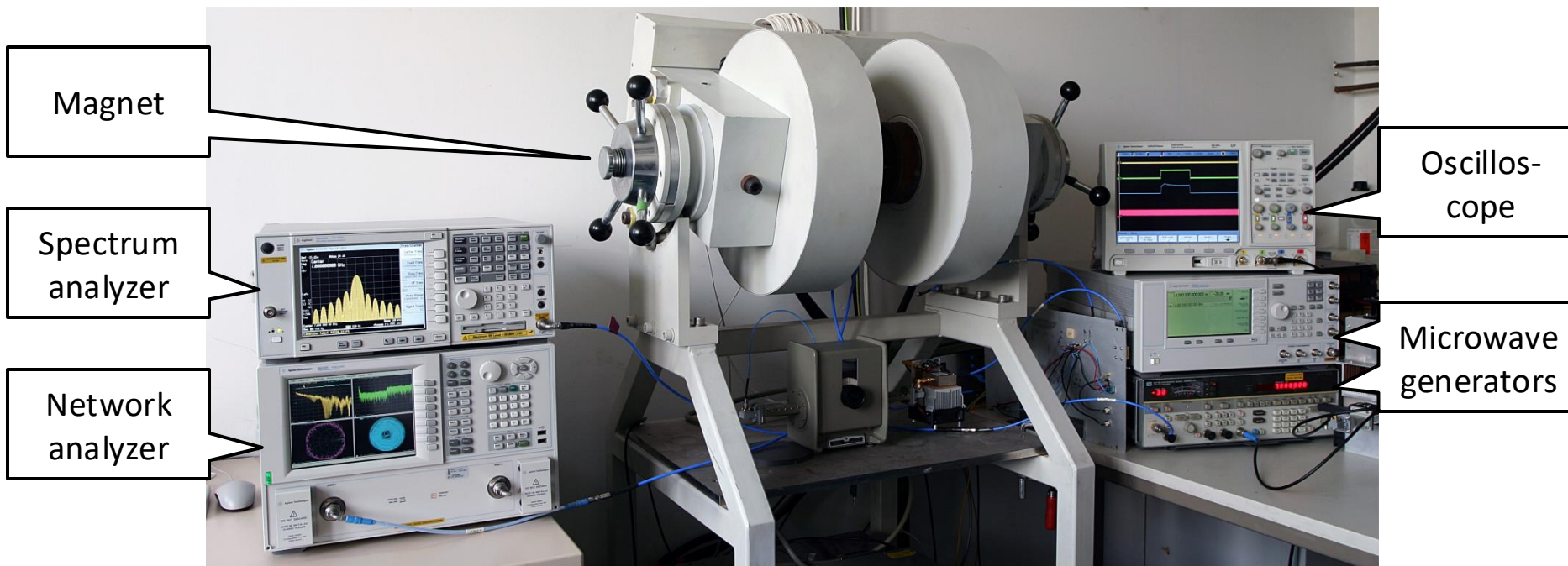


Microwave experiment

What is a microwave experiment with spin waves?

- Microwave excitation of spin waves and detection by other means (e.g. direct current/voltage, BLS, MOKE)
- Microwave input + output experiments → transmission and reflection experiments

Microwave technique

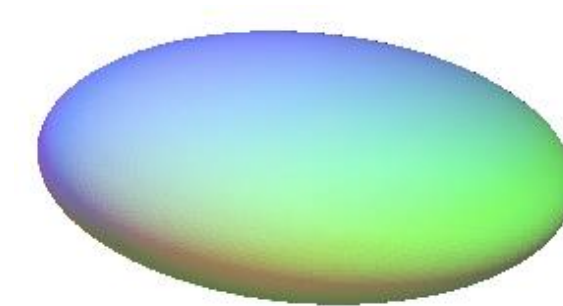


- Continuous and pulsed microwave signals having powers up to ≈ 100 W in frequency range from 1 to 20 GHz
- Precise spin-wave amplitude and phase measurements in a wide frequency range using spectrum and network analyzers
- Temporal measurements with sub-ns resolution using a broadband oscilloscope
- Microwave characterization: both linear and nonlinear dynamics of magnetization in nano-structured and in macroscopic samples

Uniform resonant oscillation of ellipsoid

Problem: demagnetizing field is most often inhomogeneous.

- only exception: ellipsoid



Magnetic field $\overset{r}{B}_{\text{int}}$ inside ellipsoid as function of external field $\overset{r}{B}_{\text{ext}}$:

$$\overset{r}{B}_{\text{int}} = \overset{r}{B}_{\text{ext}} - \mu_0 \overset{t}{N} \overset{r}{M} = \overset{r}{B}_{\text{ext}} + \overset{r}{B}_{\text{demag}}$$

with N : demagnetizing tensor, symmetric, $N_{xx} + N_{yy} + N_{zz} = 1$,

$\overset{r}{B}_{\text{demag}}$: demagnetizing field,

$N_{xy} = 0$ for $x \neq y$ if $\overset{r}{B}_{\text{ext}}$ principal axis of ellipsoid.

Condition of equilibrium for equilibrium saturation magnetization $\overset{r}{M}_0$ in energy minimum:

$$\overset{r}{M}_s \times \left(\overset{r}{B}_{\text{ext}} - \mu_0 \overset{t}{N} \overset{r}{M}_s \right) = 0$$

Equation of motion: $\frac{1}{\gamma} \frac{\partial \overset{r}{M}}{\partial t} = -\overset{r}{M} \times \overset{r}{B}_{\text{int}}$, and, with $\overset{r}{M}(t) = \overset{r}{M}_s + \overset{r}{m}_0 e^{i\omega t}$, $\overset{r}{B}_{\text{ext}} \parallel \overset{r}{M}_s \parallel \hat{e}_z$

in linear approximation:

$$\begin{aligned} (i\omega + \gamma N_{xy} \mu_0 M_s) m_x &+ \gamma (B_{\text{ext}} - N_{zz} \mu_0 M_s + N_{yy} \mu_0 M_s) m_y = 0 \\ -\gamma (B_{\text{ext}} - N_{zz} \mu_0 M_s + N_{xx} \mu_0 M_s) m_x &+ (i\omega - \gamma N_{xy} \mu_0 M_s) m_y = 0 \end{aligned}$$

Uniform resonant oscillation of ellipsoid in oblique field

Eigen frequencies:

$$\omega_0^2 = (\omega_B + \gamma\mu_0 N_{xx} M_s)(\omega_B + \gamma\mu_0 N_{yy} M_s) - \gamma^2 \mu_0^2 N_{xy}^2 M_s^2$$

with $\omega_B = \gamma(B_{\text{ext}} - \mu_0 N_{zz} M_s)$

Example: \vec{B}_e along one of the principal axes $\Rightarrow \vec{N}$ is diagonal

$$\Rightarrow \omega_0^2 = \gamma^2 (B_{\text{ext}} + \mu_0 (N_{xx} - N_{zz}) M_s) (B_{\text{ext}} + \mu_0 (N_{yy} - N_{zz}) M_s)$$

Thin film in xy -plane magnetized along \hat{z} -axis, i.e., $N_{xx} = N_{yy} = 0$, $N_{zz} = 1$

$$\Rightarrow \omega_0 = \gamma (B_{\text{ext}} - \mu_0 M_s), \text{ i.e. internal field is external field minus saturation magnetization}$$

Thin film in xz -plane magnetized along \hat{z} -axis

$$\Rightarrow \omega_0 = \gamma \sqrt{B_{\text{ext}} (B_{\text{ext}} - \mu_0 M_s)}, \text{ i.e., internal field is geometric means of the two field}$$

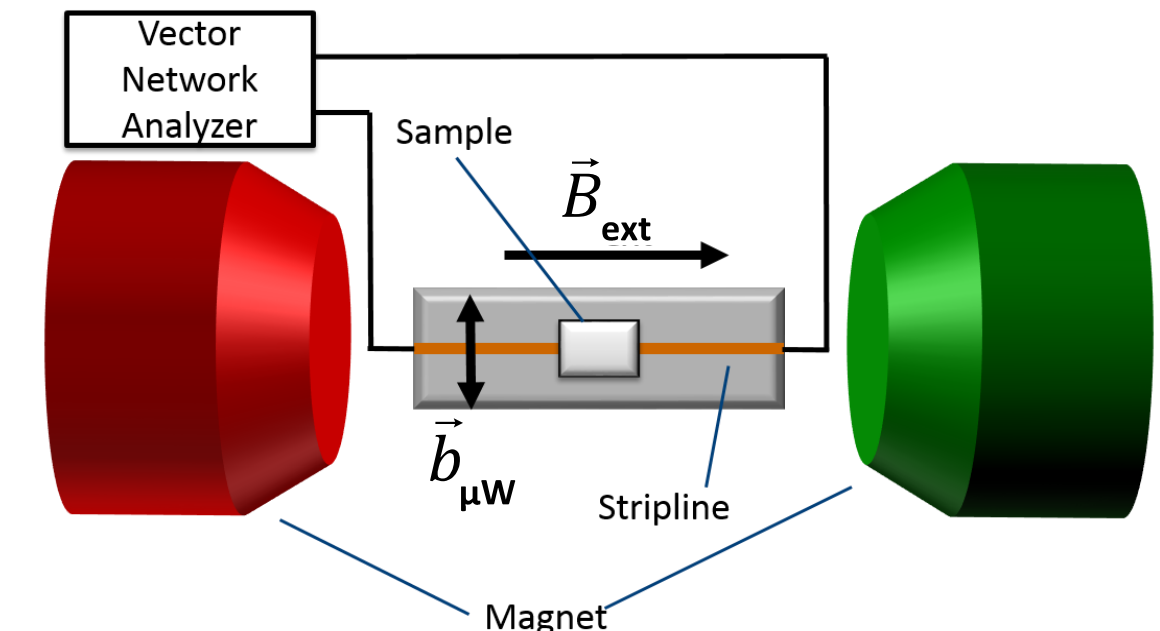
components acting on the magnetization B_{ext} and $B_{\text{ext}} - \mu_0 M_s$
(named stiffening fields).

Ferromagnetic Resonance

FMR is a measurement method at microwave frequency

Experiment:

- Sample is uniformly magnetized in a static magnetic field \vec{B}_{ext}
- Alternating microwave field $\vec{b}_{\mu\text{W}}$ with fixed frequency is applied to the sample in perpendicular direction to \vec{B}_{ext} → forced precession of magnetization vector
- Sweeping of \vec{B}_{ext}
- Experimental realization:
Sample
 - in microwave cavity, or
 - on micro-stripline

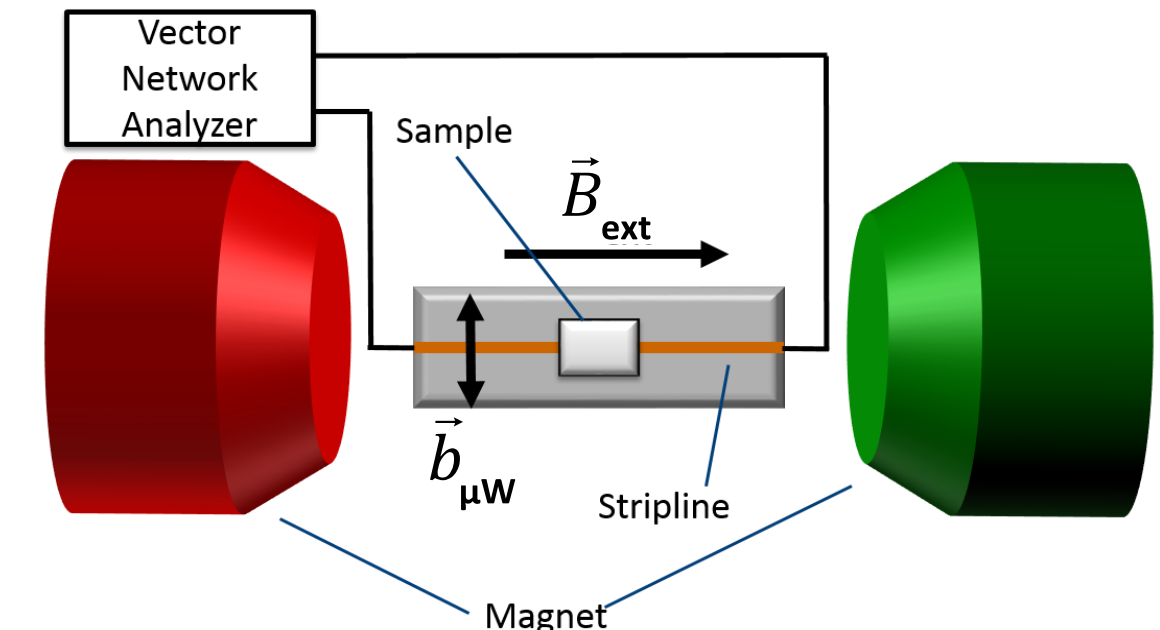


Ferromagnetic Resonance

Resonance frequency:

$$\omega_{\text{res}} = \frac{ge}{2m_e} \sqrt{\left(\frac{2K}{M_s} + B_{\text{ext}} + \mu_0 M_s (N_{yy} - N_{xx}) \right) \left(\frac{2K}{M_s} + B_{\text{ext}} + \mu_0 M_s (N_{zz} - N_{xx}) \right)}$$

anisotropy field external field demagnetizing field

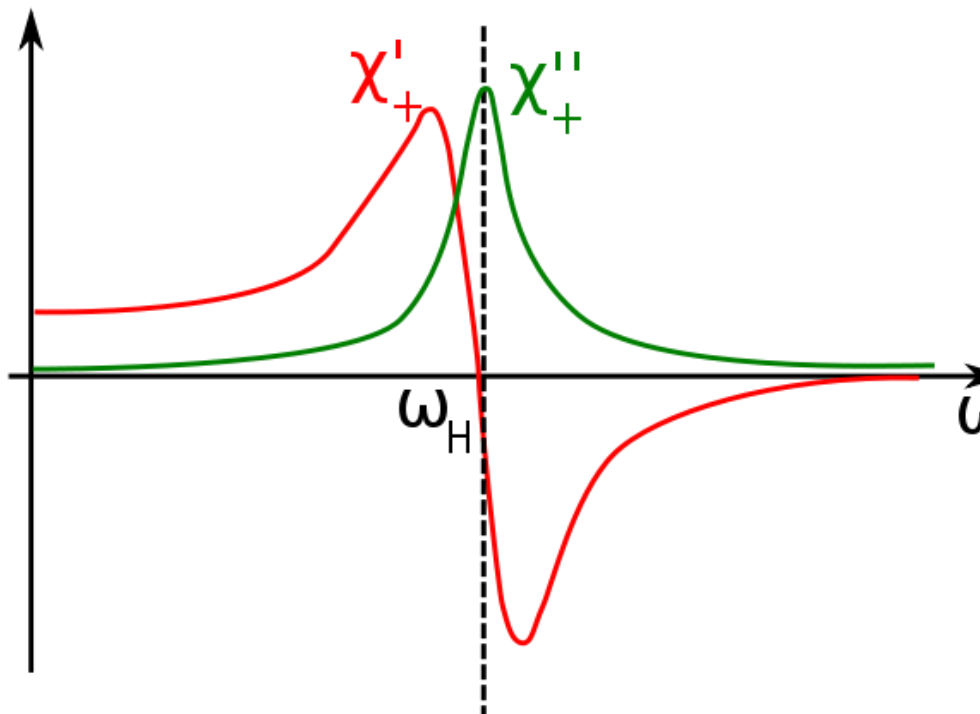


Ferromagnetic Resonance

Measurement:

Change in microwave signal intensity as a function of applied magnetic field $\frac{dI_{\text{microwave}}}{dB_{\text{ext}}}$

or microwave frequency $\frac{dI_{\text{microwave}}}{d\omega} \rightarrow$ determination of the **complex dynamic susceptibility**:



Source: Wikipedia Commons

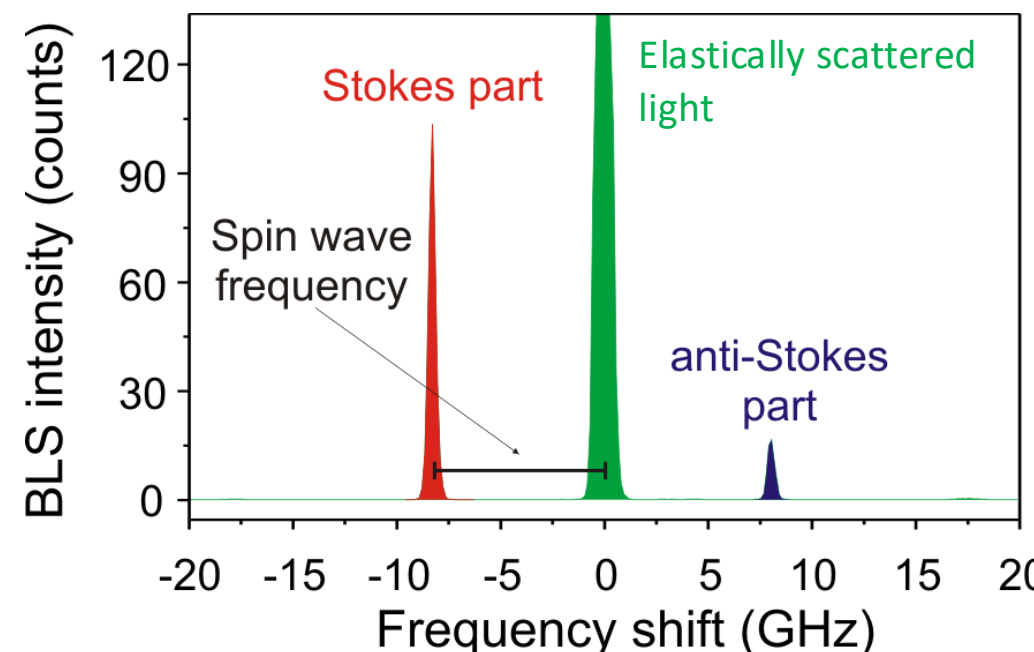
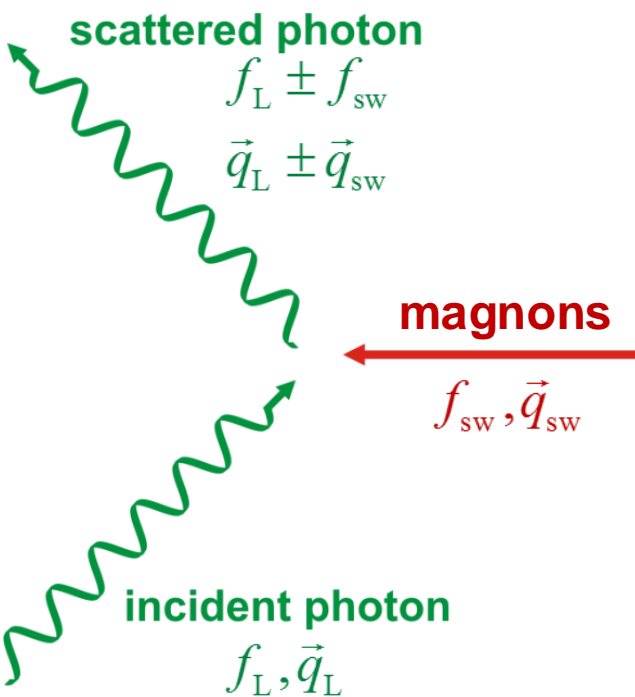
Brillouin light scattering (BLS) spectroscopy

- Inelastic scattering of photons from spin waves:

$$f_{\text{scattered L}} = f_L \pm f_{\text{sw}}$$

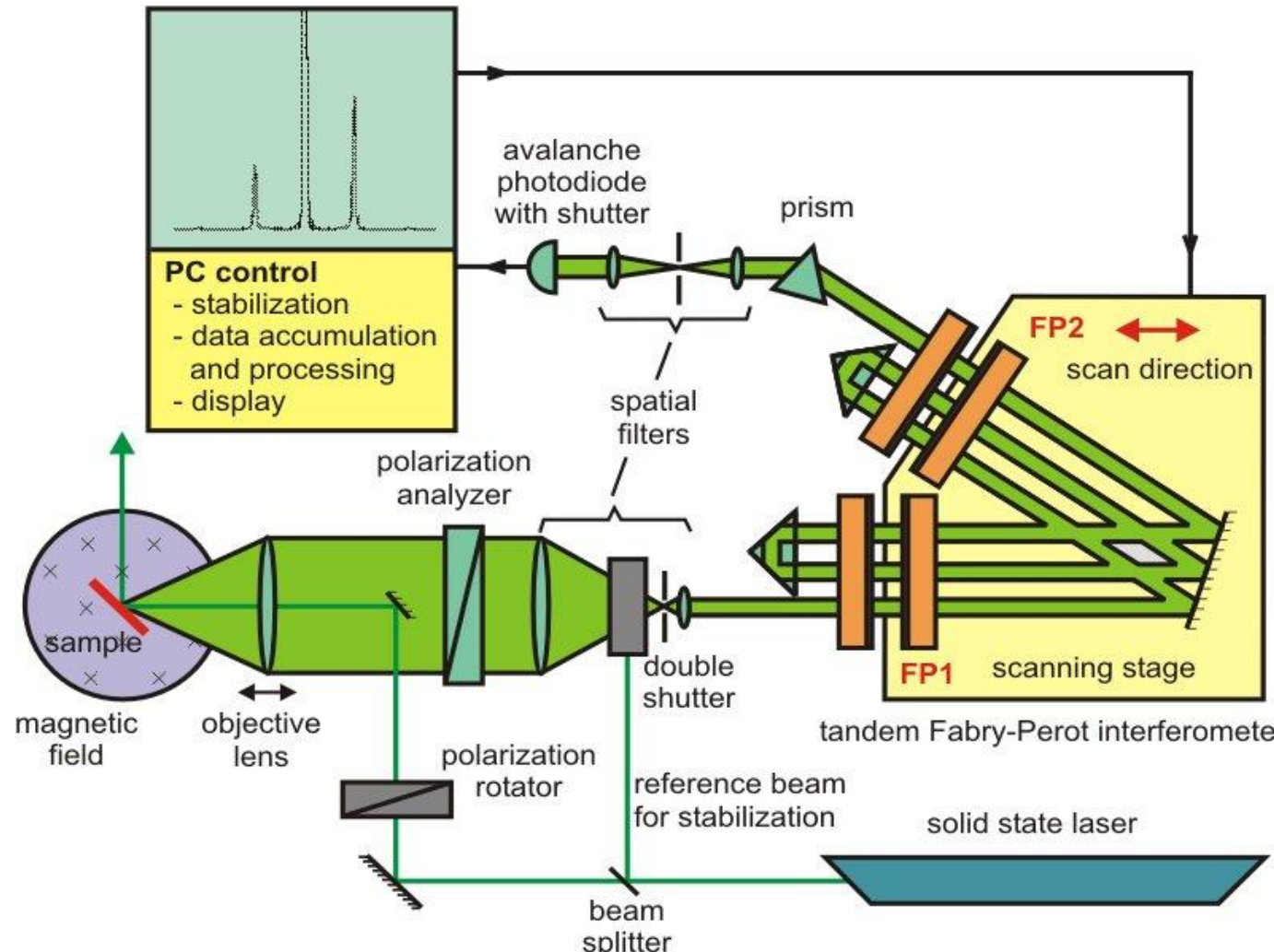
$$\vec{q}_{\text{scattered L}} = \vec{q}_L \pm \vec{q}_{\text{sw}}$$

- Intensity of the scattered light is proportional to magnon density

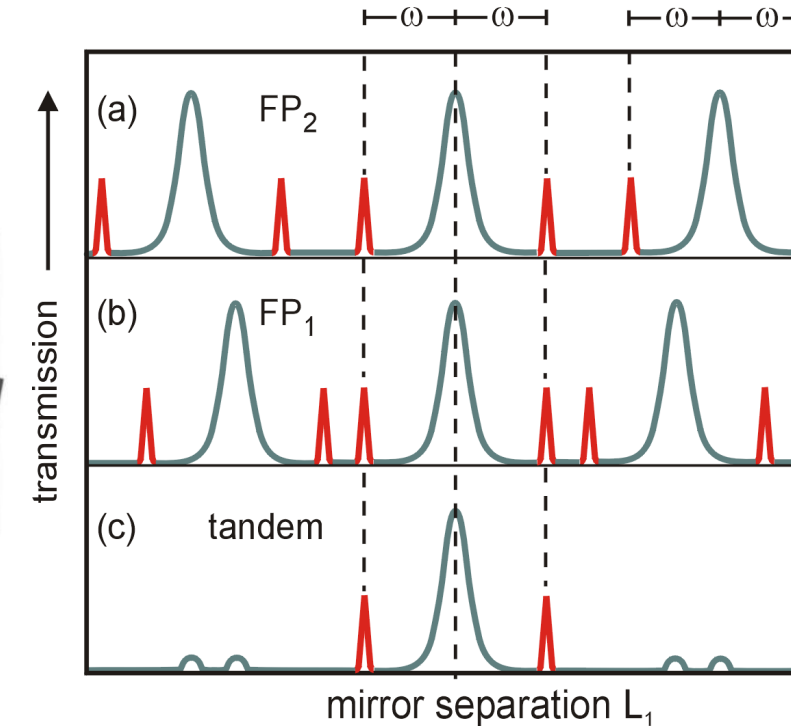
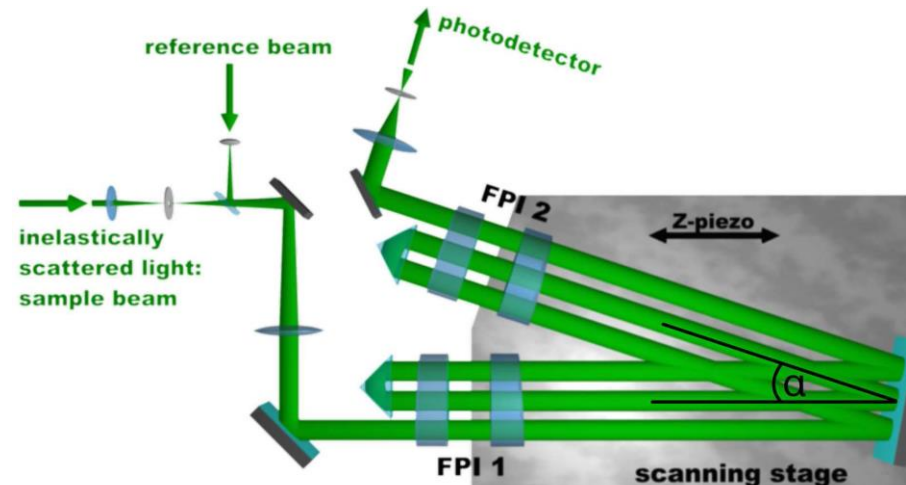


Brillouin light scattering spectrometer

high-resolution interferometry with high contrast
for measurements of acoustic phonons and spin waves



Brillouin light scattering spectrometer

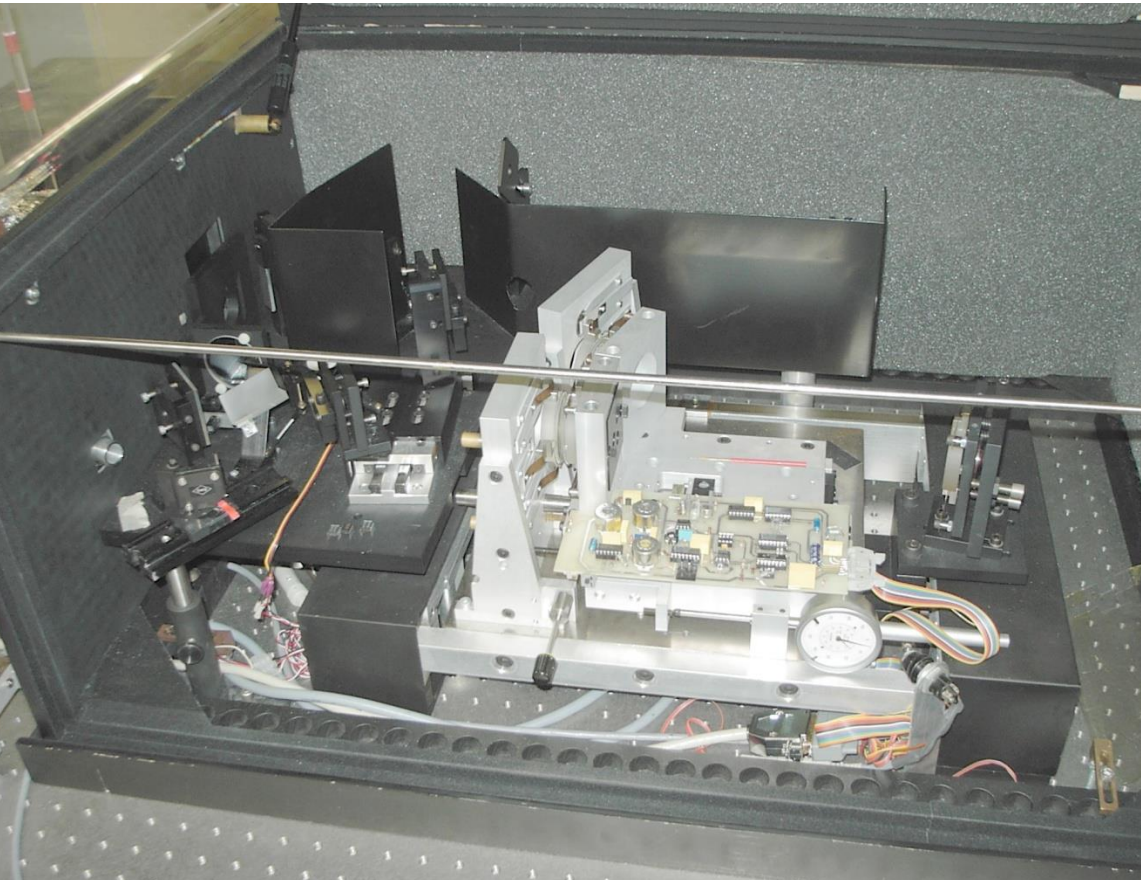


- etalon in transmission if mirror separation L is:
- $$L = n \lambda_{\text{Laser}} / 2$$
- suppression of neighboring orders if mirror separations L_1, L_2 of both etalons:

$$L_2 = L_1 \cos \alpha$$

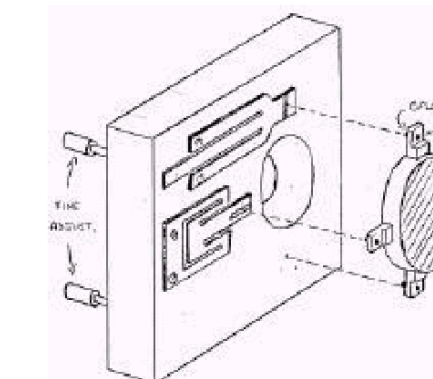
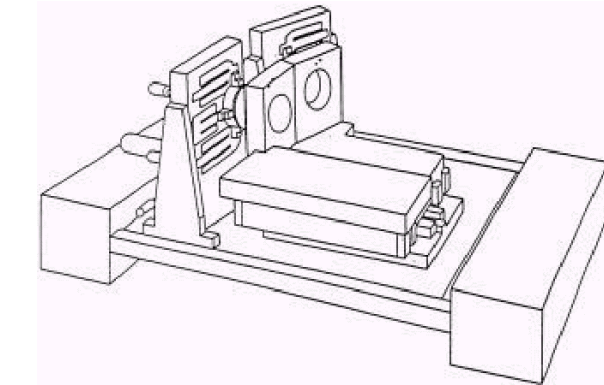
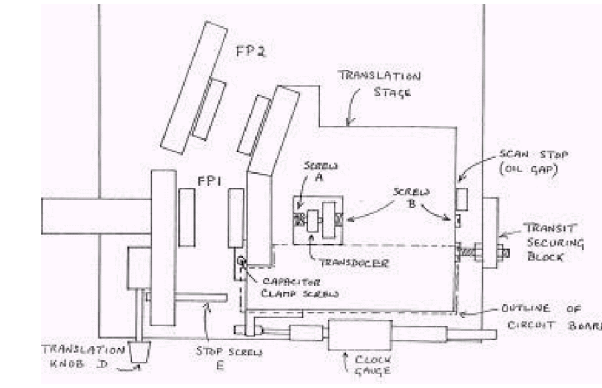
α : angle between etalon axes

Brillouin light scattering spectrometer

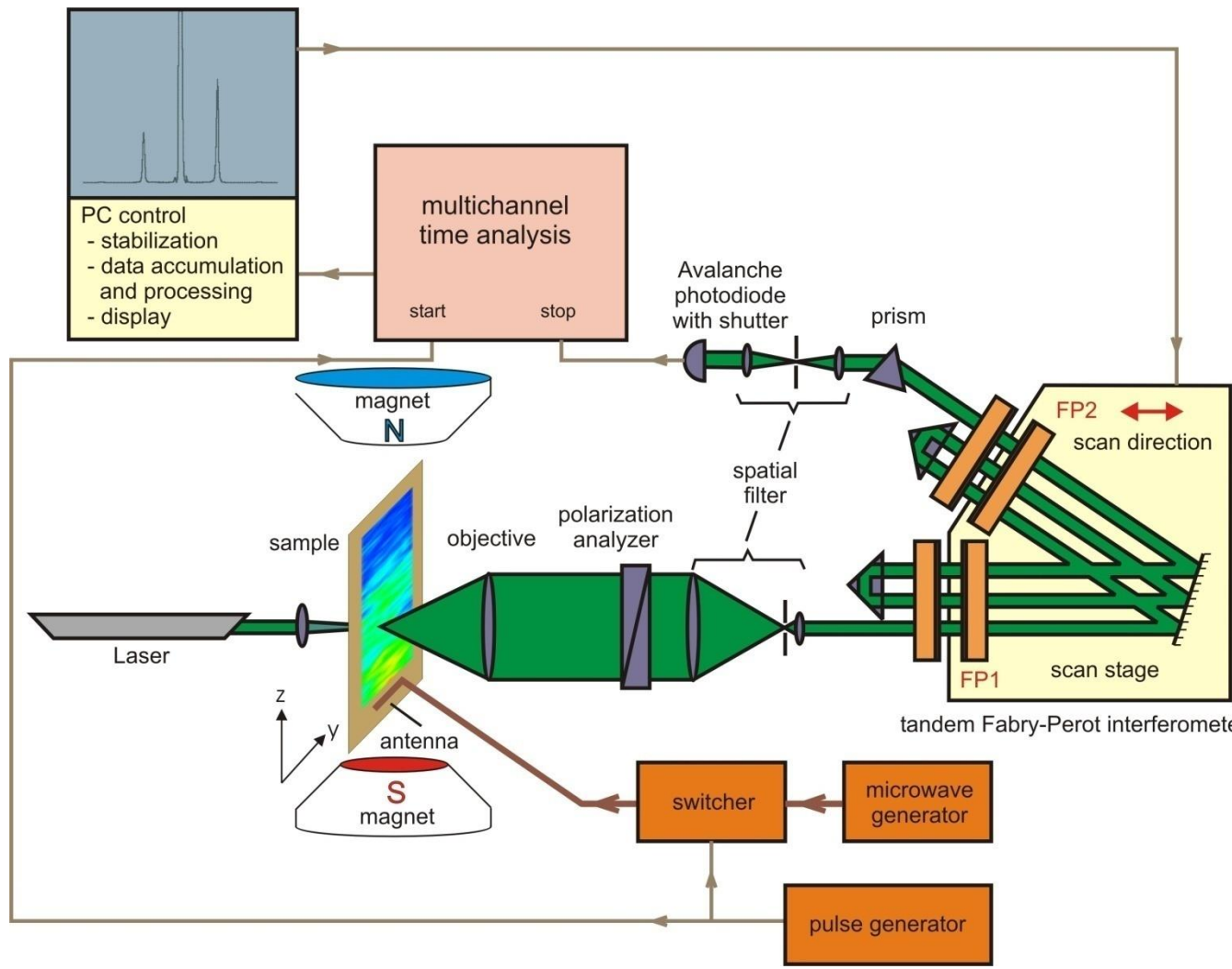


Tandem Fabry-Pérot Interferometer

Sketch of mechanical stage and mirror mounts
(from John Sandercock's 1993 manual)



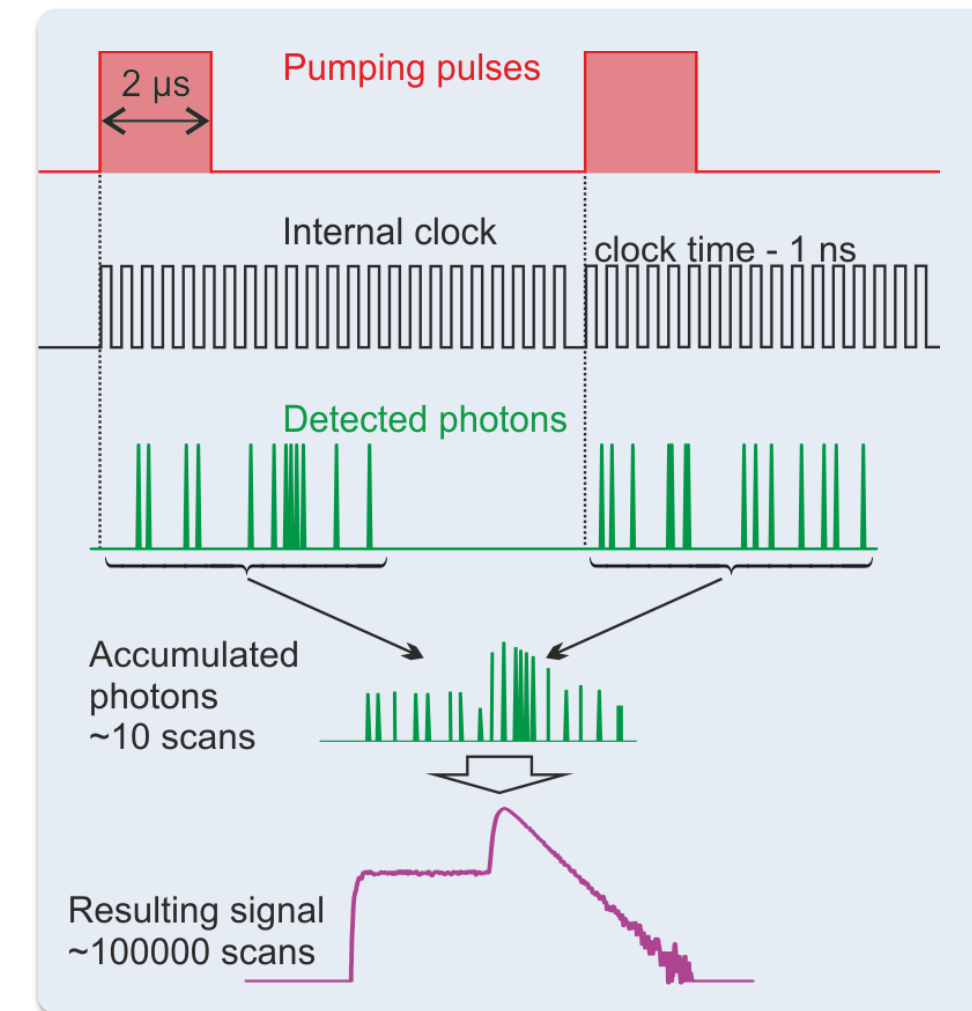
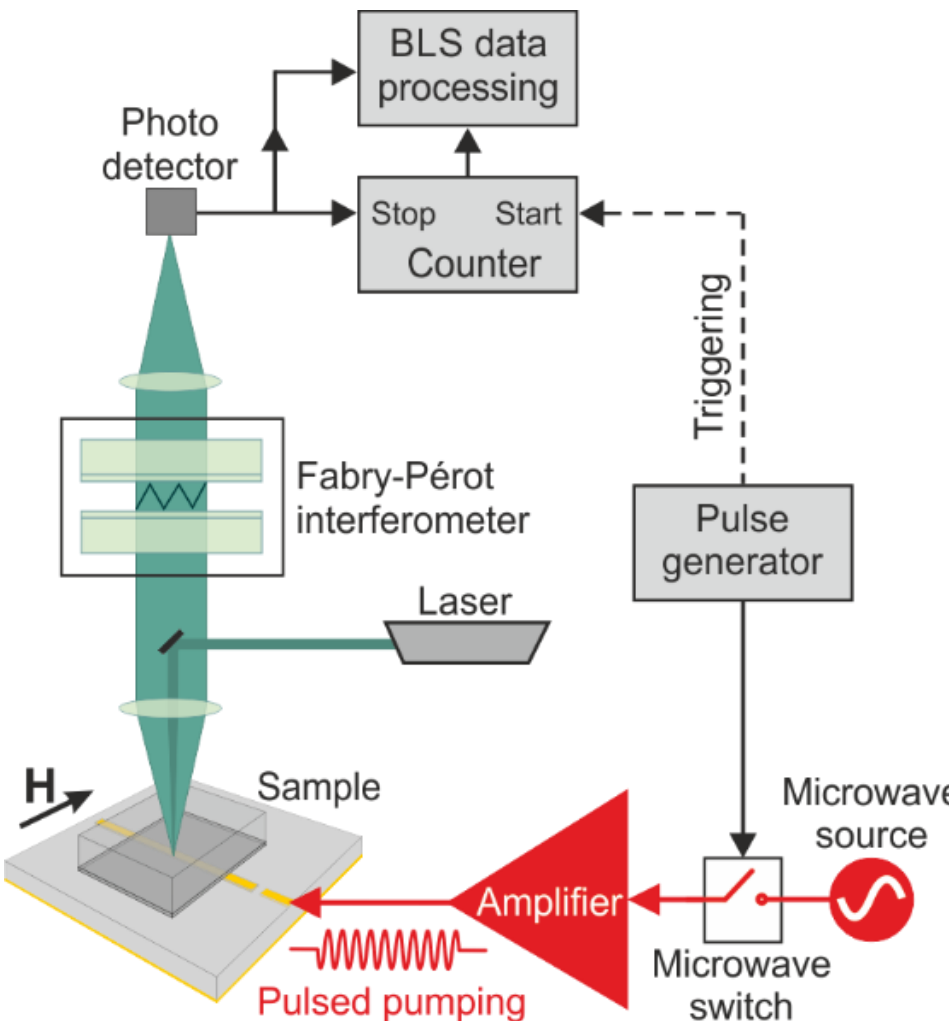
Time- and space-resolved Brillouin light scattering spectroscopy



spatial resolution: 40 μm
time resolution: 1 ns
dynamic range: >60 dB

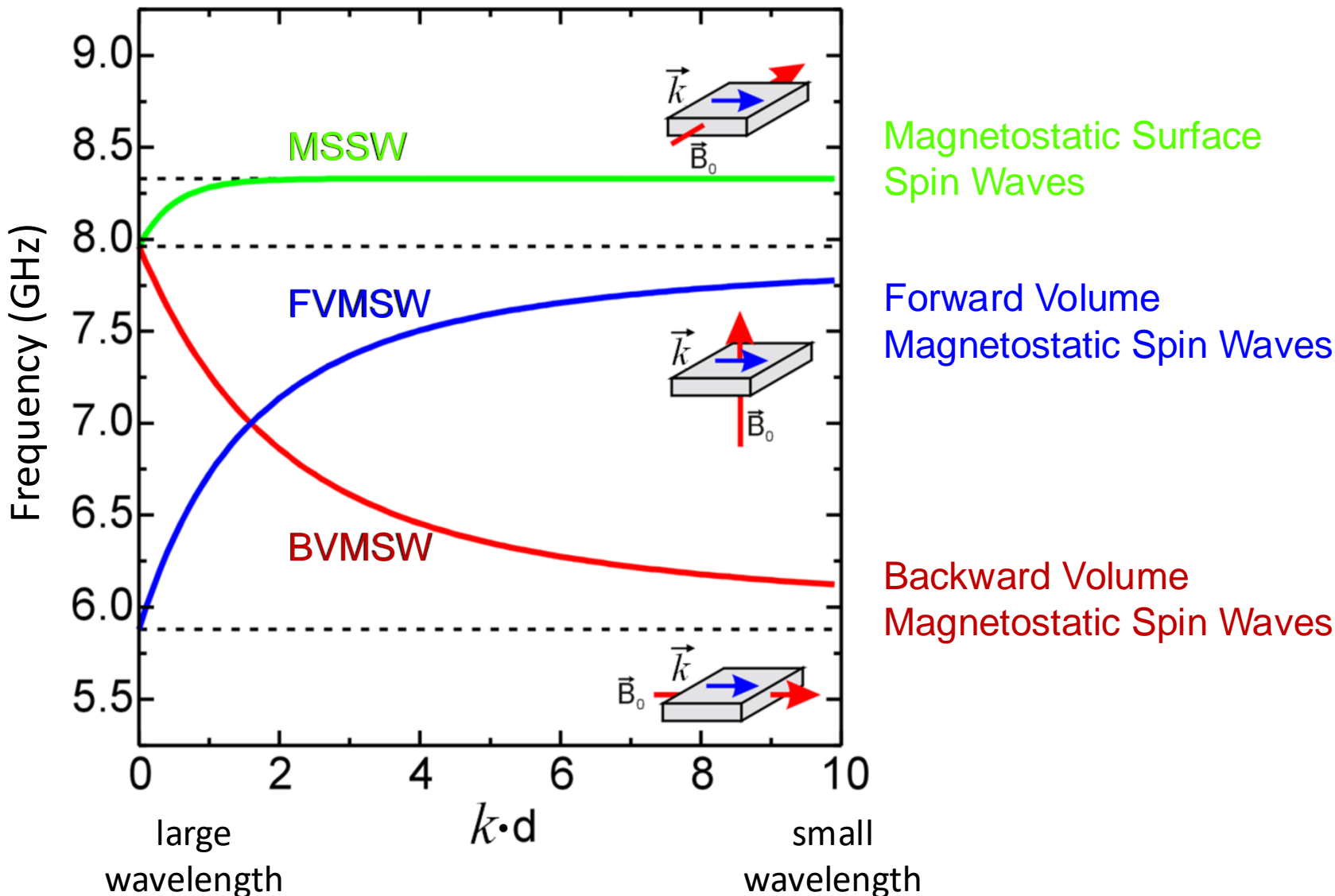
O. Büttner *et al.*, Phys. Rev. B **61**, 11576 (2000)

Time-resolved BLS spectroscopy

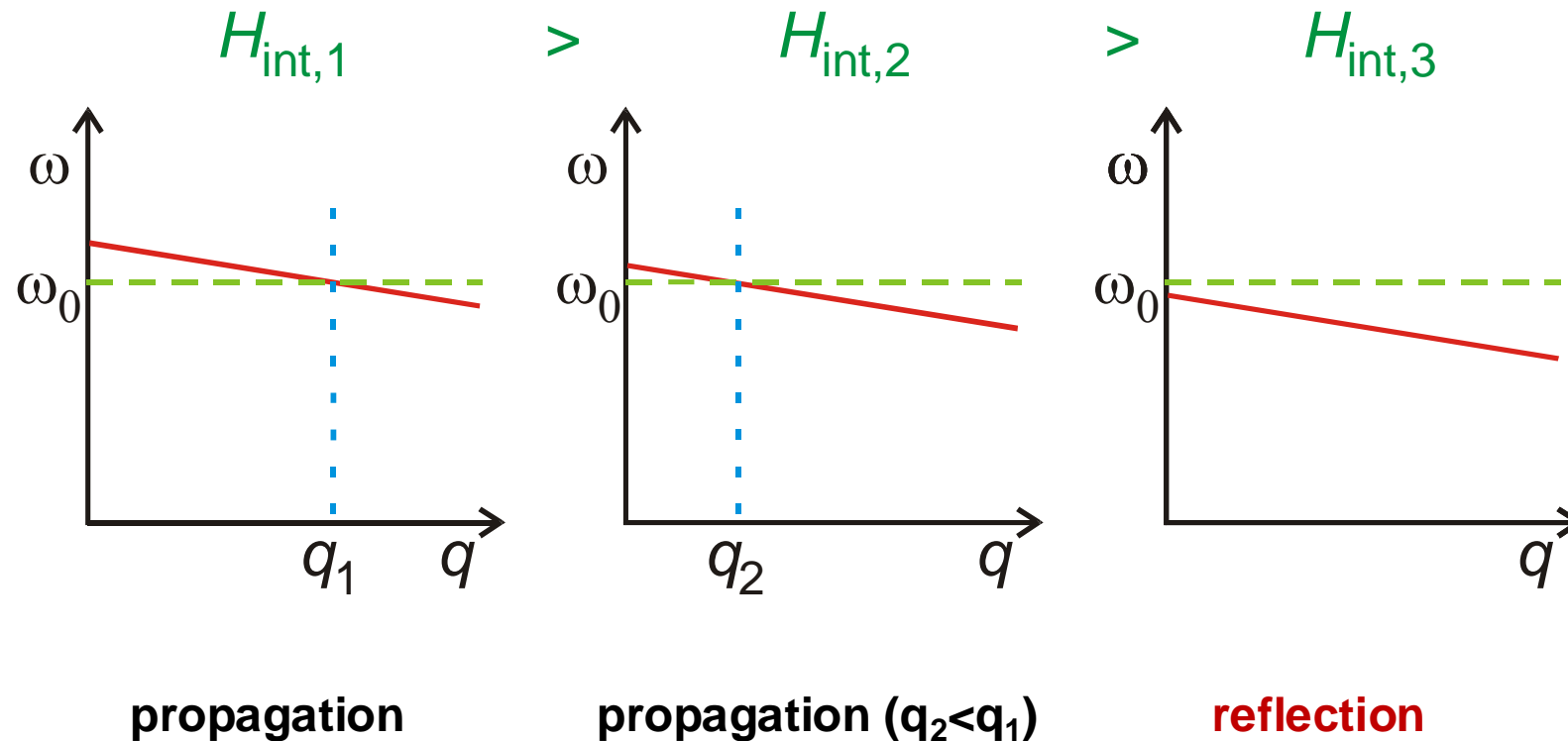


Time resolution: 1 ns

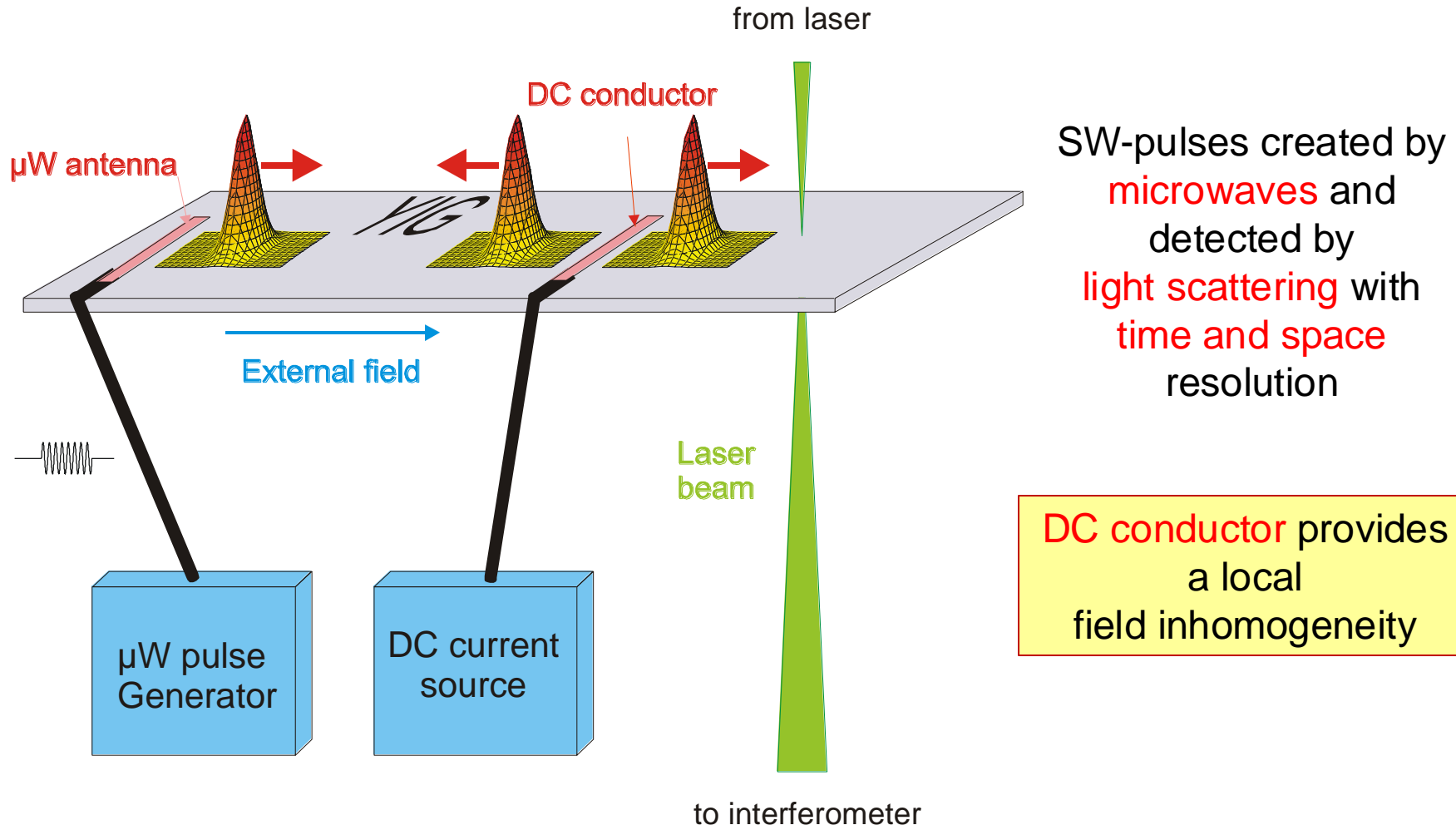
Dipolar spin waves



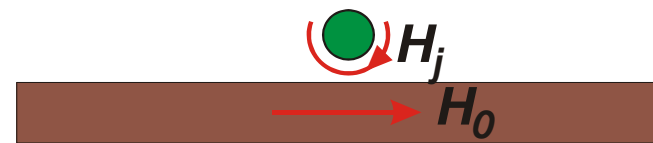
Motion of a spin wave packet in varying field



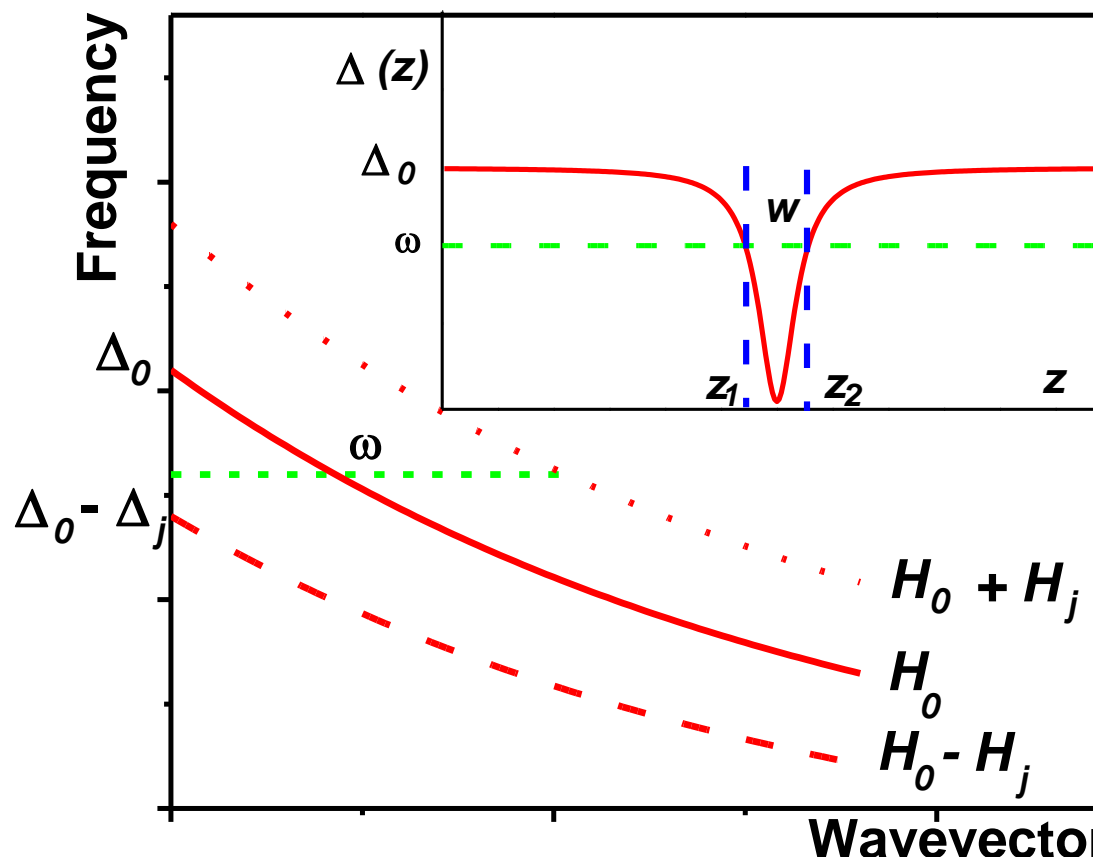
Real-time observation of spin wave propagation



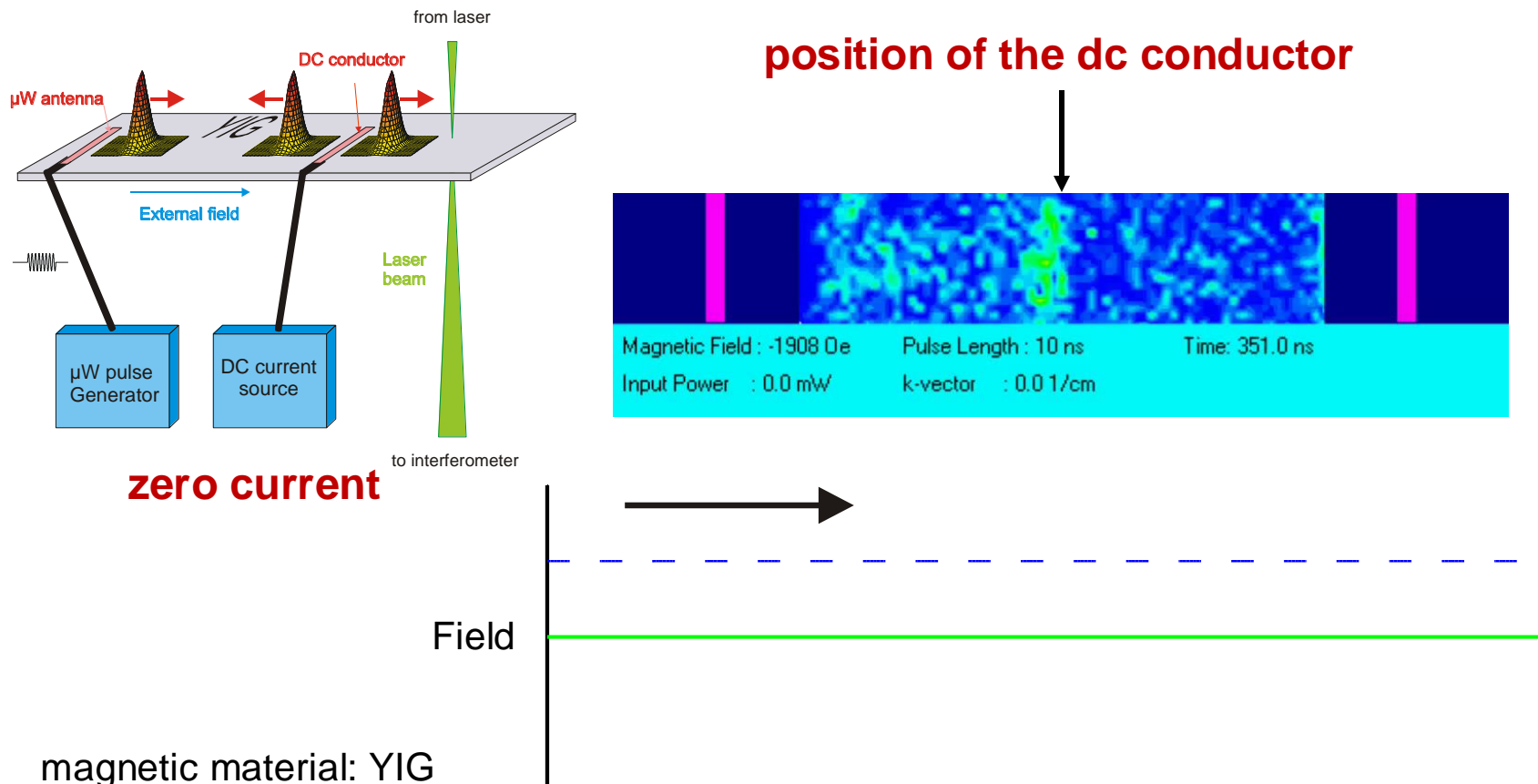
Spin wave tunneling



Δ : zero-wavevector gap

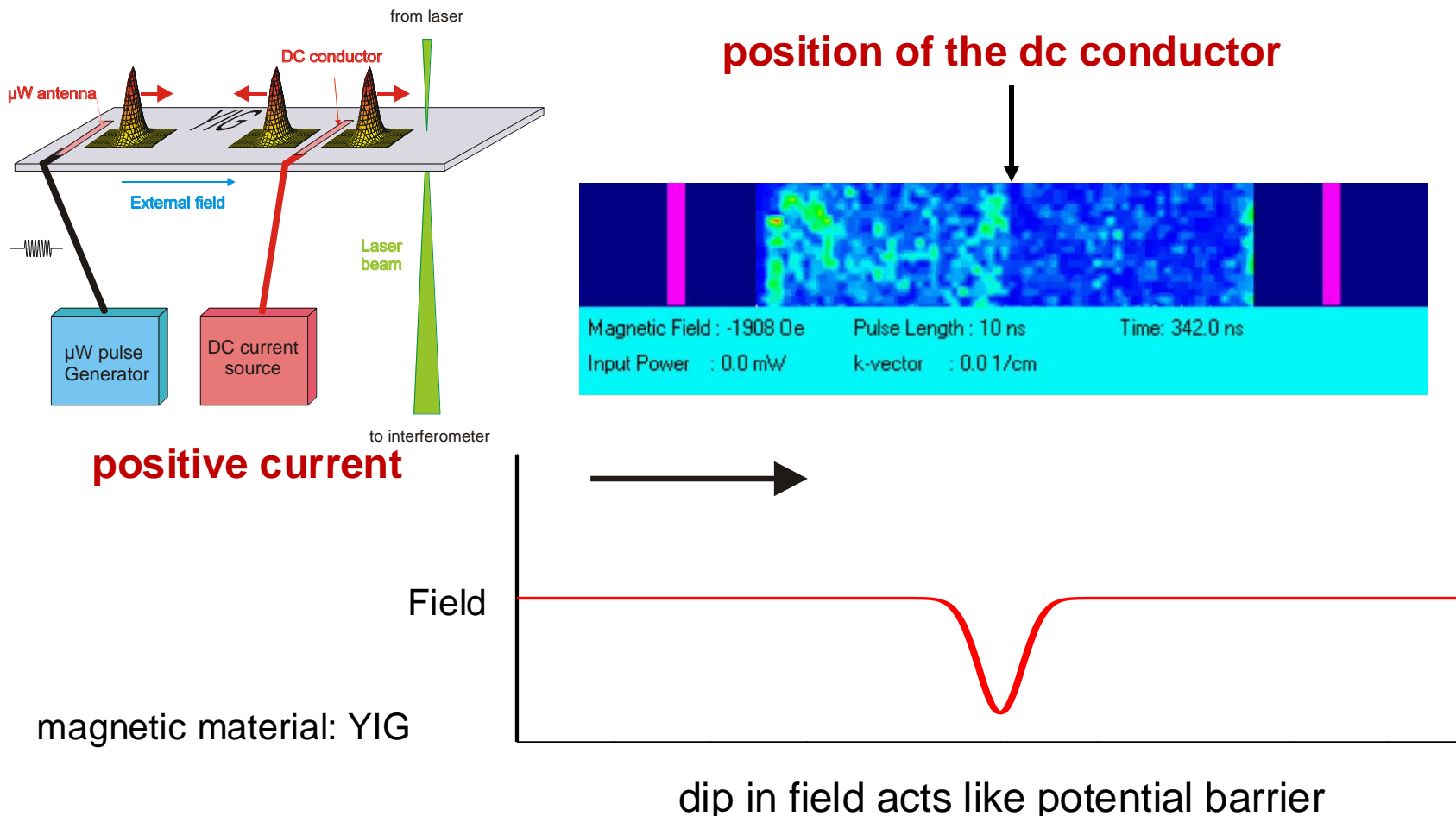


Spin wave pulse propagation



S.O. Demokritov *et al.*, Phys. Rev. Lett. **93**, 047201 (2004)

Spin wave pulse propagation



Potential barrier: reflection and tunneling

S.O. Demokritov *et al.*, Phys. Rev. Lett. **93**, 047201 (2004)

Reflection of spin wave at barrier and spin wave tunneling

Carrier frequency:
7.125 GHz

Bias field:
1836 Oe

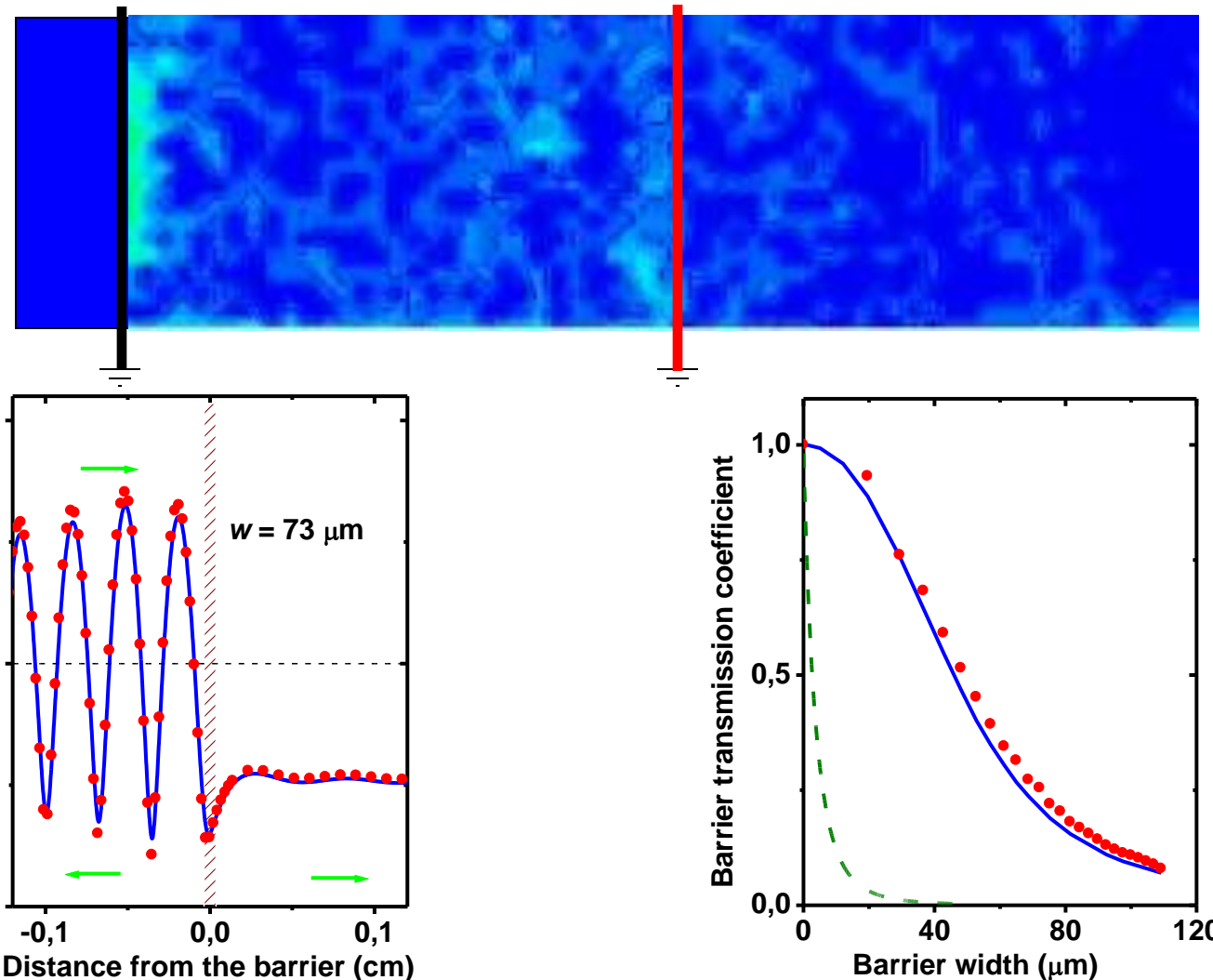
Wave number:
112 rad/cm

Group velocity:
 ≈ 30 km/s

Film thickness:
5.7 μm

Scan region:
 $6.0 \times 1.8 \text{ mm}^2$

Logarithmic scale



A. A. Serga *et al.*, Appl. Phys. Lett. **94**, 112501 (2009)

Non-exponential decrease of spin wave intensity with barrier size

Spin-wave Fabry-Perot interferometer

Carrier frequency:
7.125 GHz

Bias field:
1836 Oe

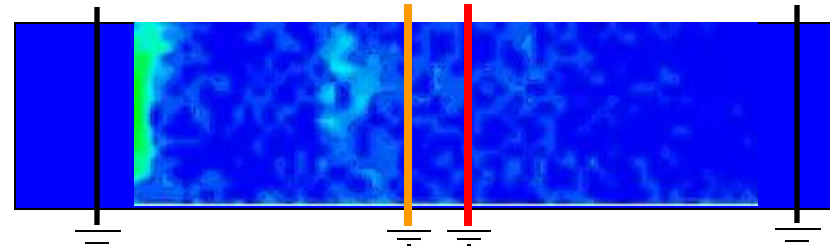
Wave number:
112 rad/cm

Group velocity:
 ≈ 30 km/s

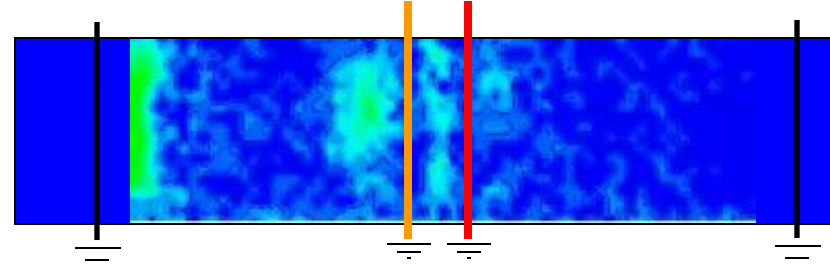
Film thickness:
 $5.7 \mu\text{m}$

Scan region:
 $6.0 \times 1.8 \text{ mm}^2$

Logarithmic scale



Short SW pulse
18 ns



Long SW pulse
40 ns

Spin-wave tunneling through mechanical gap

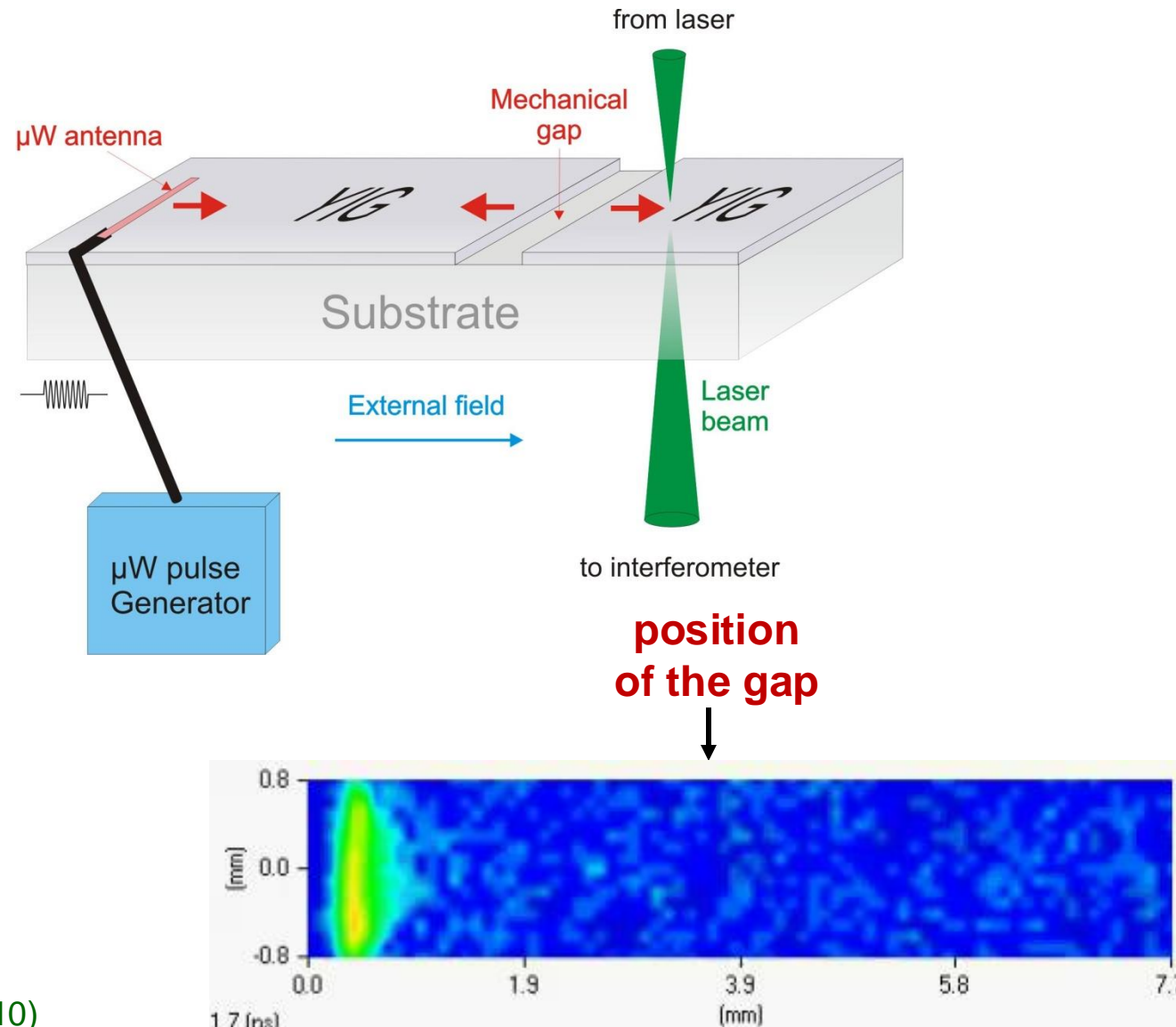
Film thickness:
 $6 \mu\text{m}$

Gap width:
 $20 \mu\text{m}$

Frequency:
 7.125 GHz

Magnetic field:
 1835 Oe

Logarithmic scale



T. Schneider *et al.*, *Europhys. Lett.* **90**, 27003 (2010)

Spin wave cavity

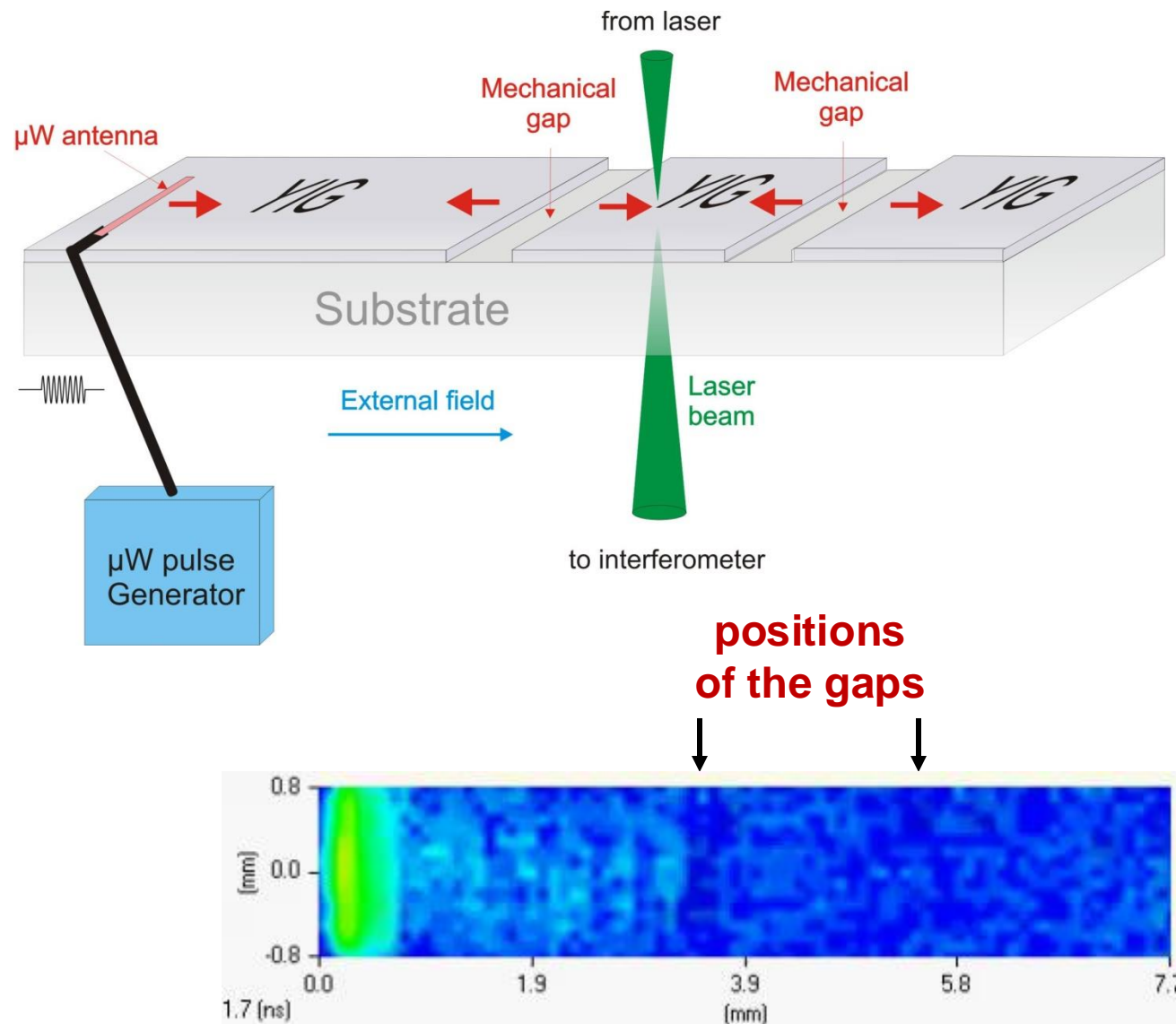
Film thickness:
 $6 \mu\text{m}$

Gap width:
 $20 \mu\text{m}$

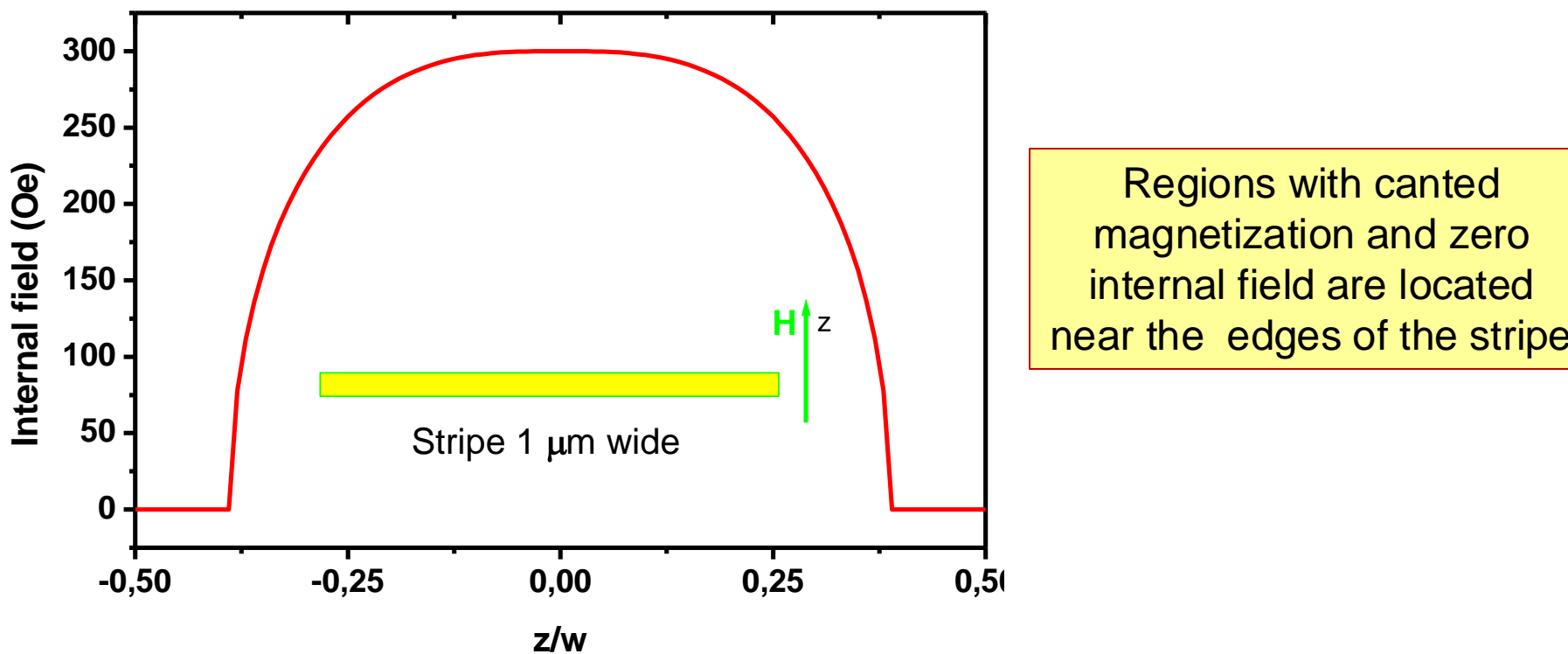
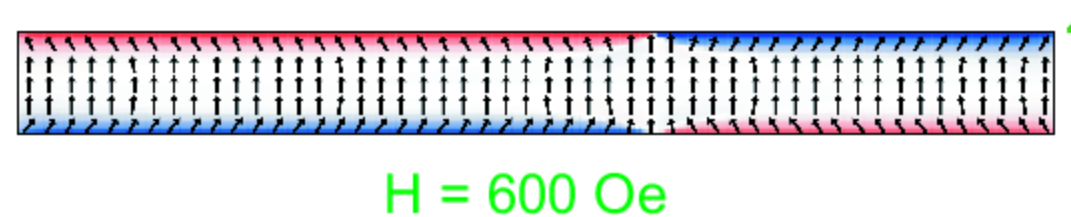
Frequency:
 7.125 GHz

Magnetic field:
 1839 Oe

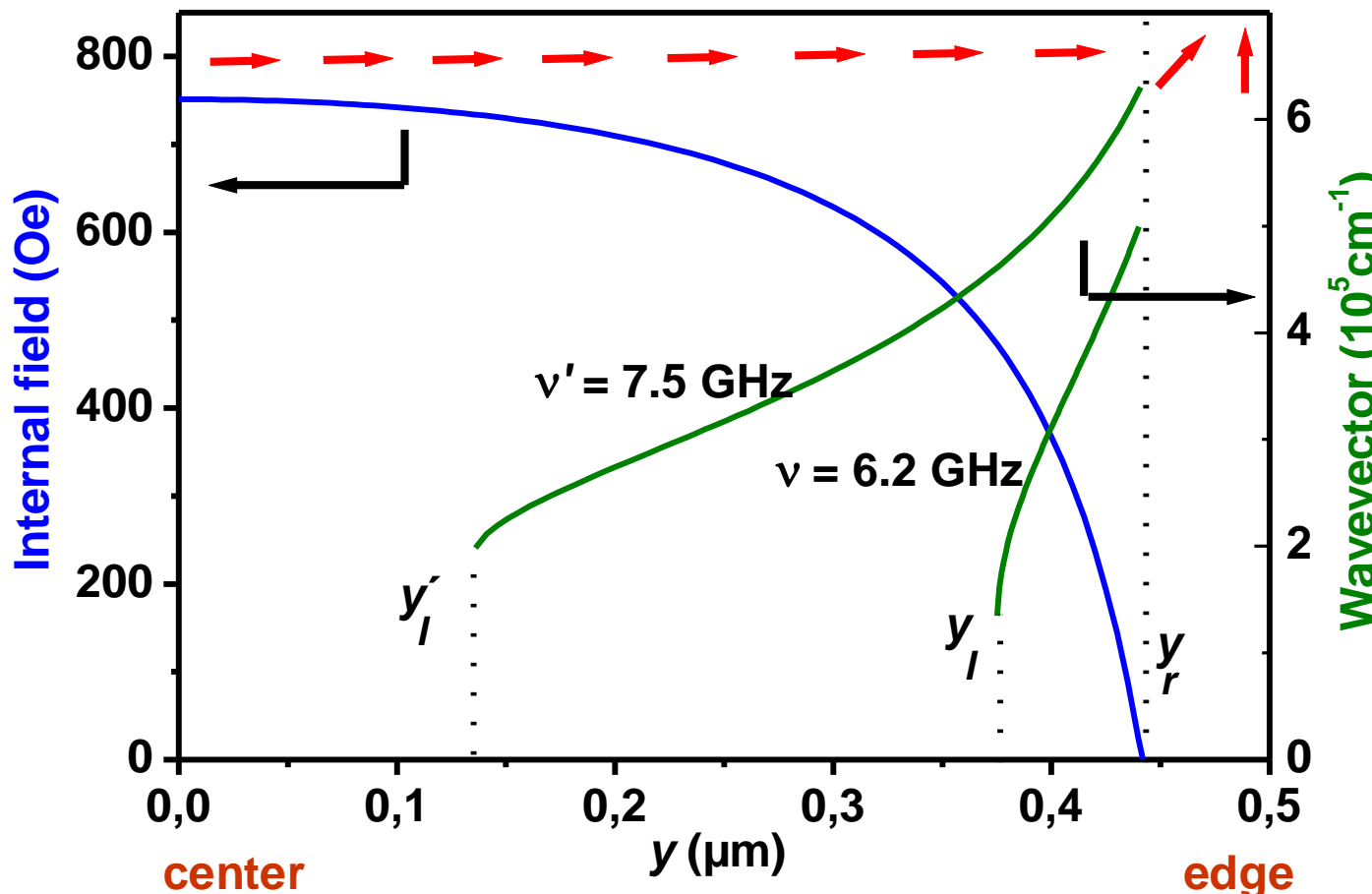
Logarithmic scale



Application: Spin waves in films with internal field distribution



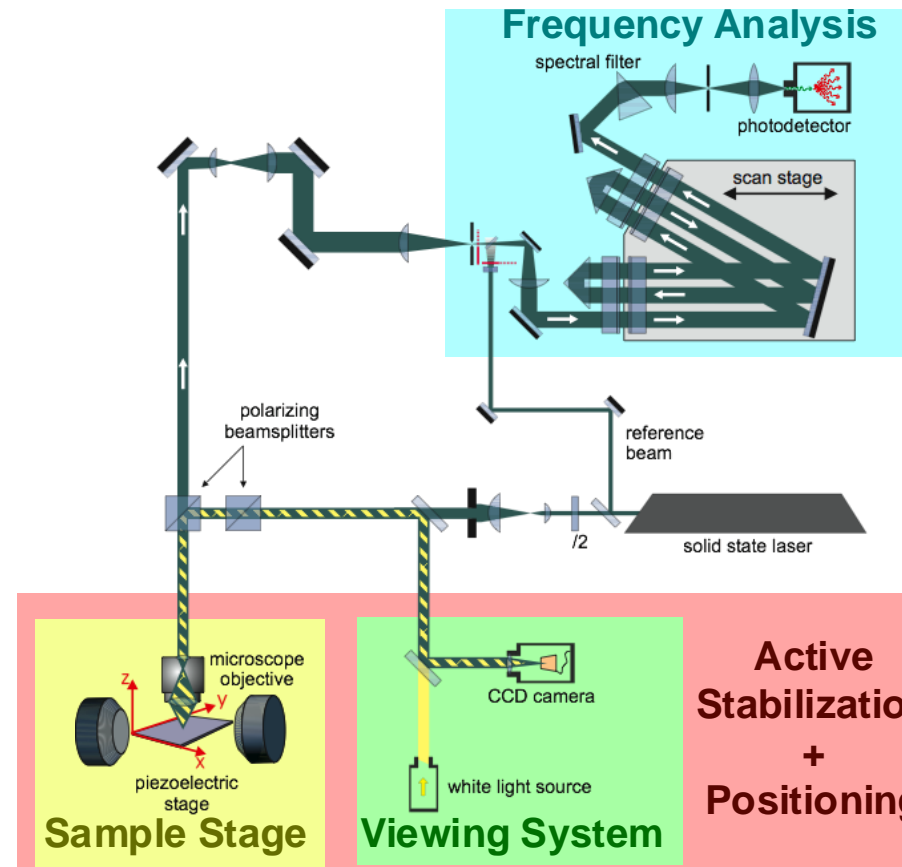
Dynamics in inhomogeneous stripe



$y_l, y_l' : \text{turning points}$

$y_r - y_l : \text{localization length}$

BLS microscopy

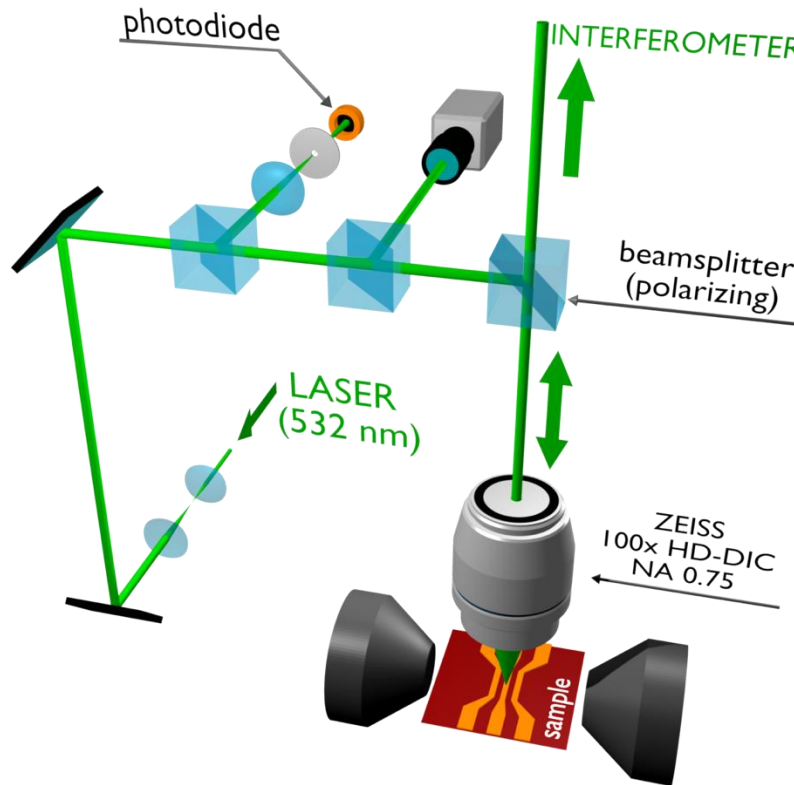


- optical resolution:
250 nm
- 2D piezo stage
- controlling sample while measuring
- frequency range:
1 GHz – 1 THz
- spectral resolution:
100 MHz
- position stability:
infinite
- accuracy:
better than 20 nm
- high reproducibility

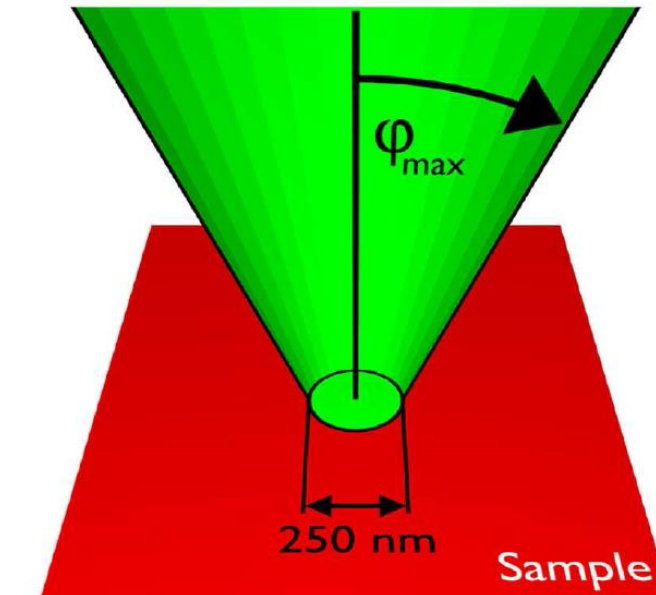
Micro-focused Brillouin light scattering spectroscopy

Experiment:

Brillouin light scattering microscopy



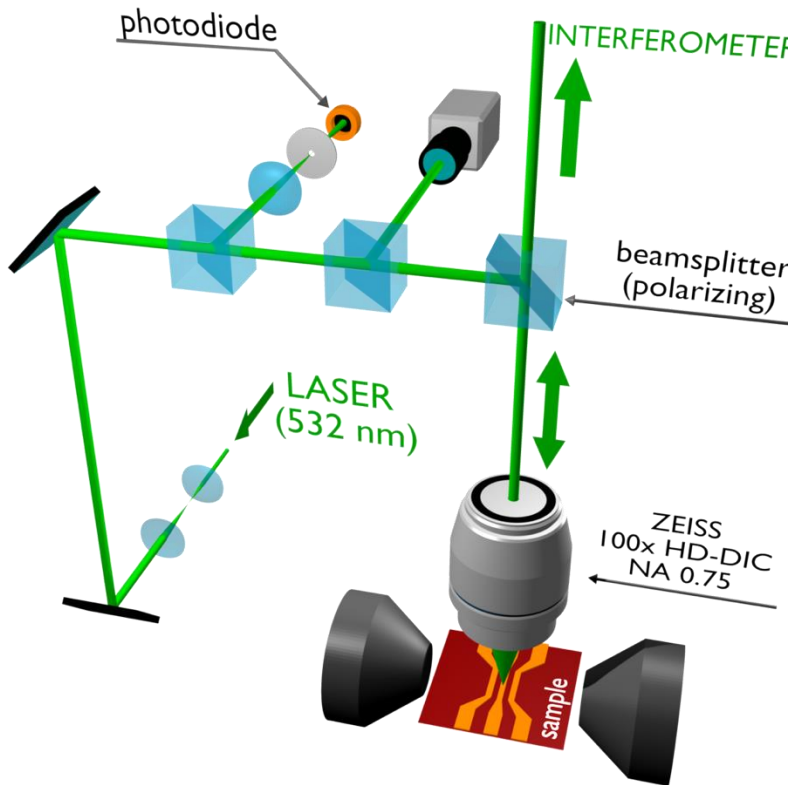
Laser focus on the sample



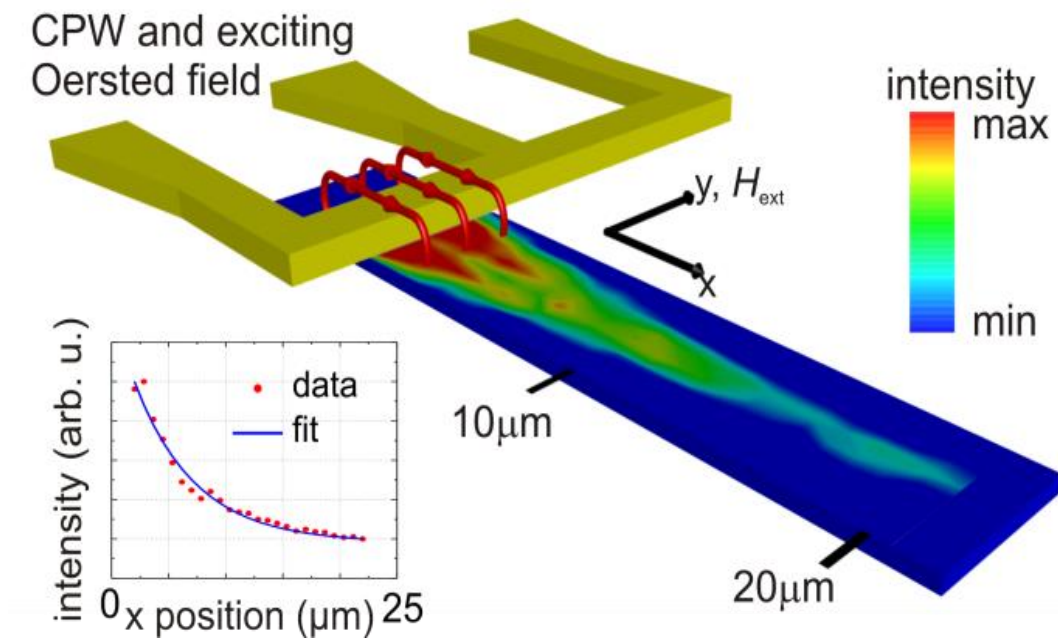
Micro-focused Brillouin light scattering spectroscopy

Experiment:

Brillouin light scattering microscopy



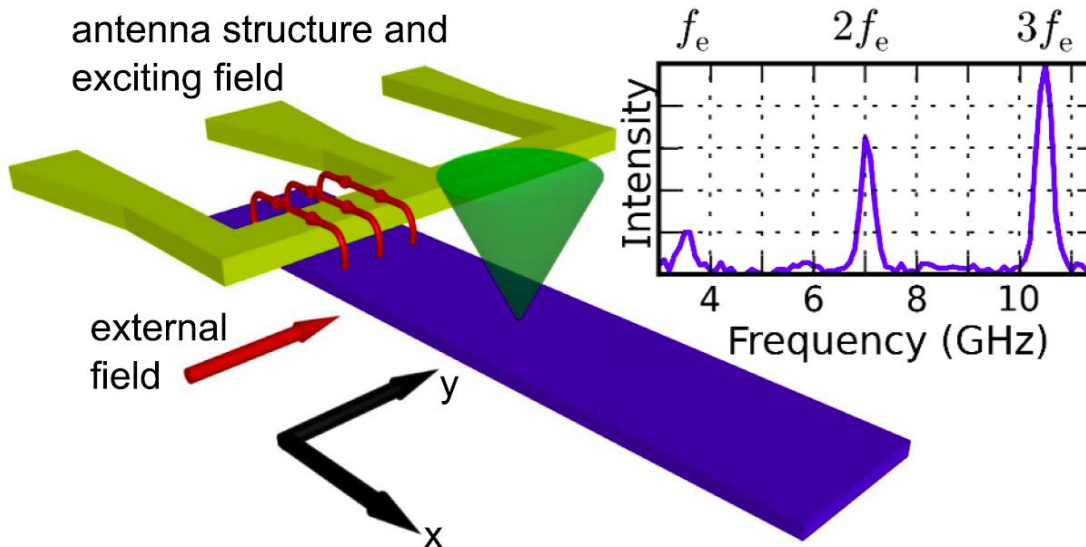
Micro-structured $\text{Co}_2\text{Mn}_{0.6}\text{Fe}_{0.4}\text{Si}$ spin-wave conduit



T. Sebastian *et al.*, Appl. Phys. Lett. **100**, 112402 (2012)

Four-magnon interactions in a spin-wave waveguide

High frequency harmonic generation

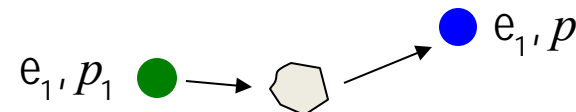


T. Sebastian et al., Phys. Rev. Lett. **110**, 067201 (2013)

(Non-)linear Processes

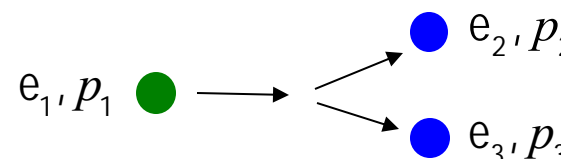
- **Linear process**

Two-magnon scattering

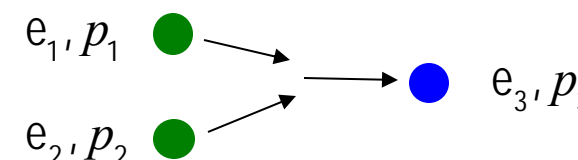


- **Nonlinear processes**

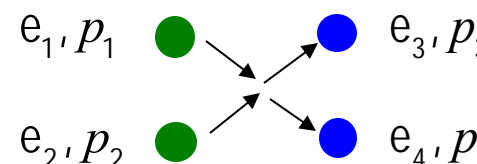
Three-magnon decay



Three-magnon confluence

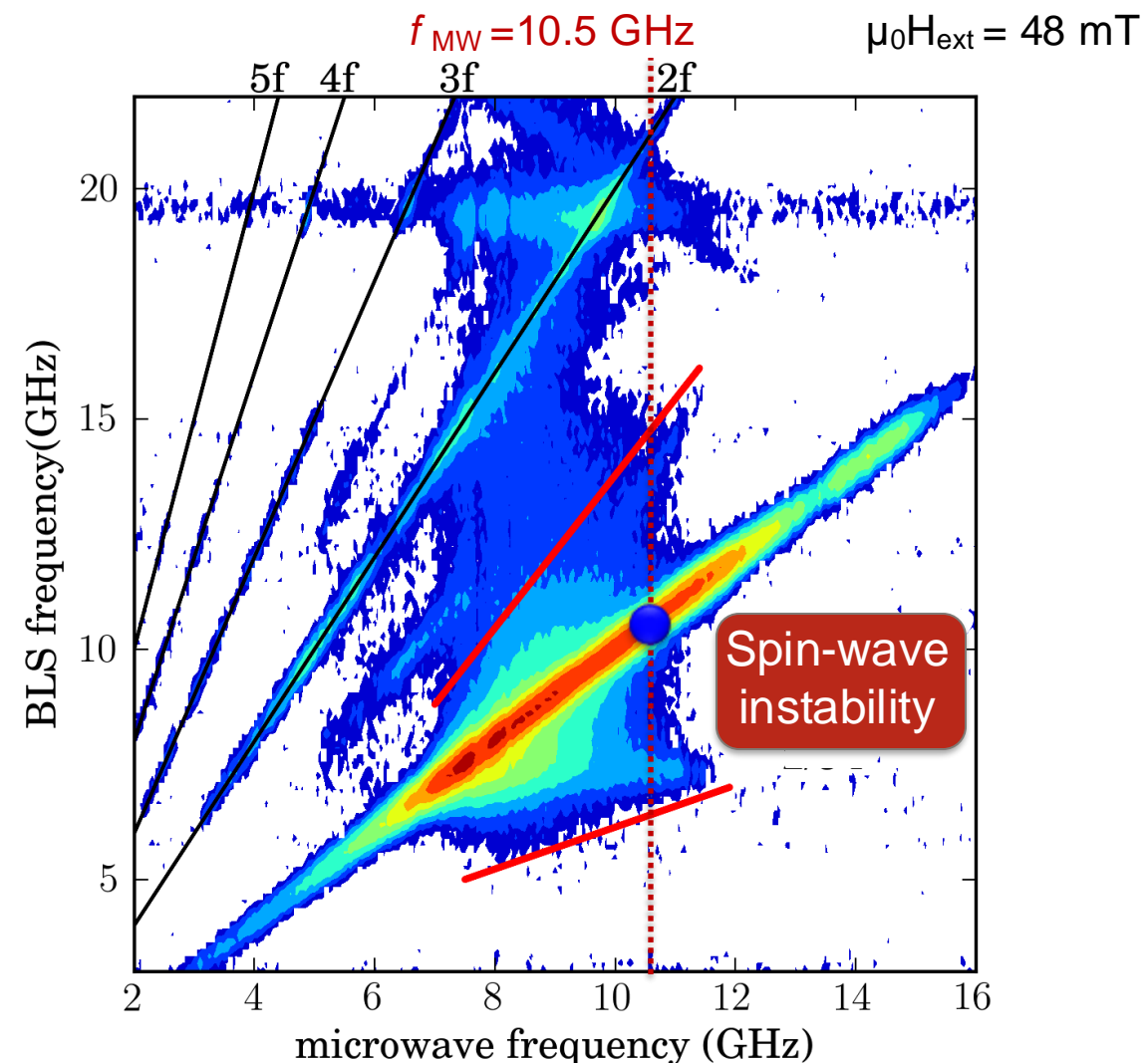
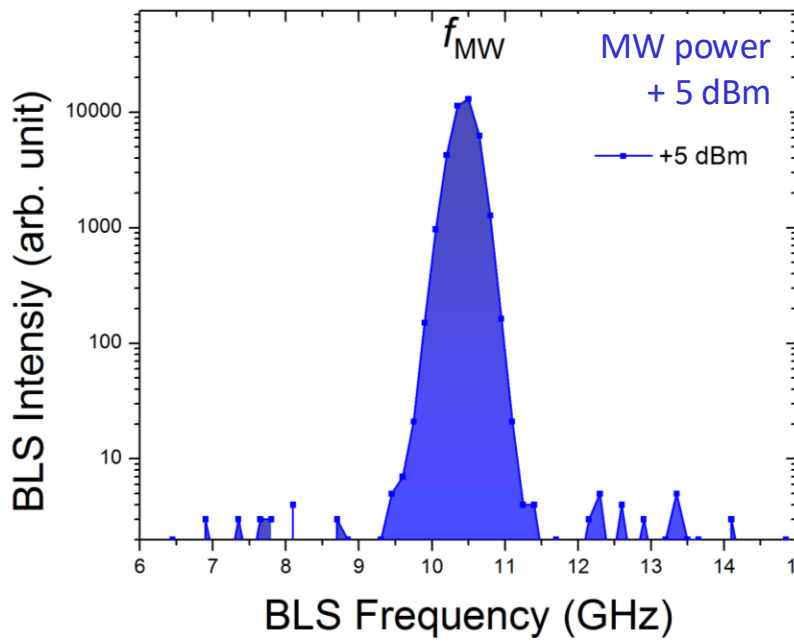


Four-magnon scattering



Four-magnon interactions in a spin-wave waveguide

Linear regime

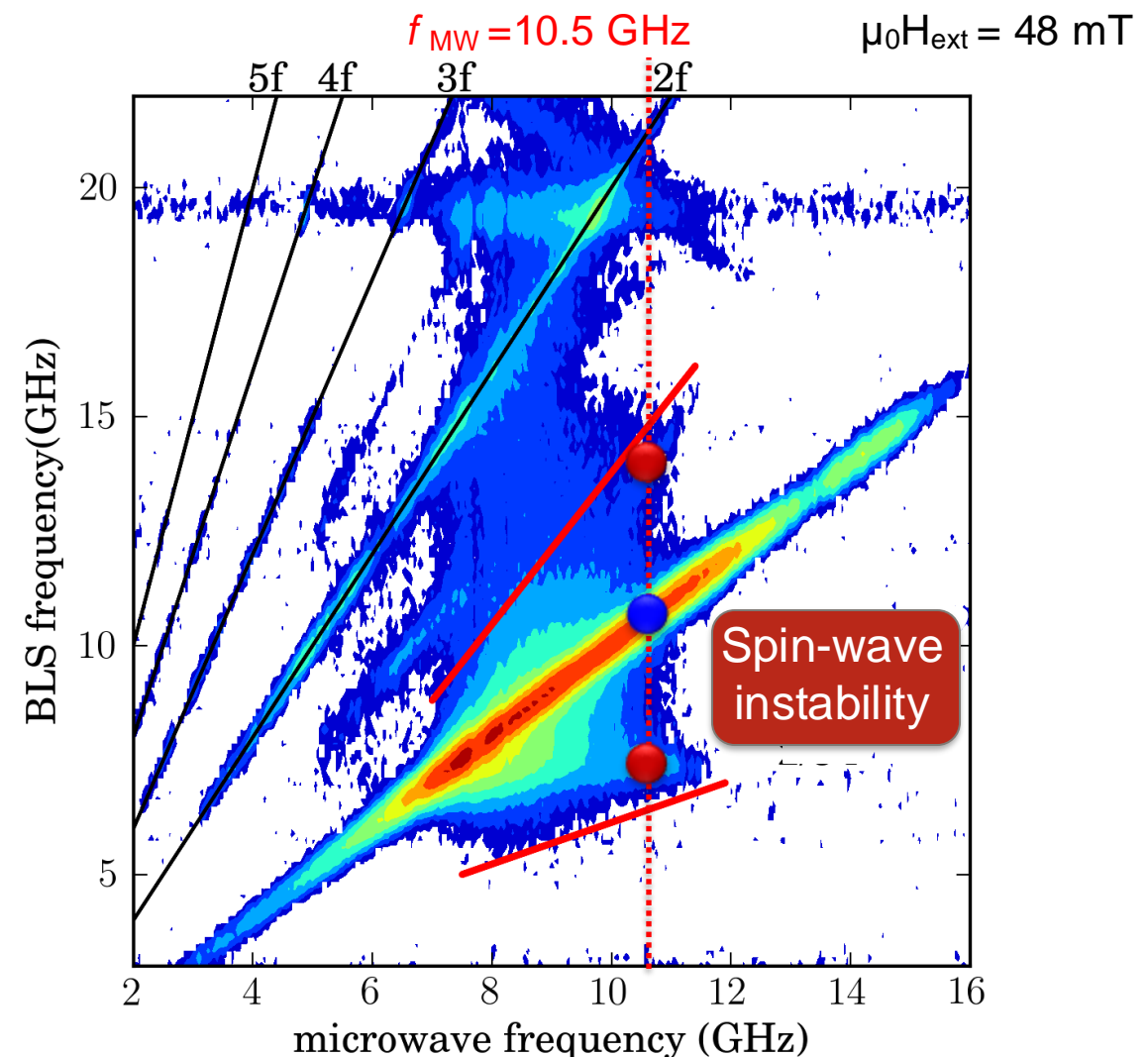
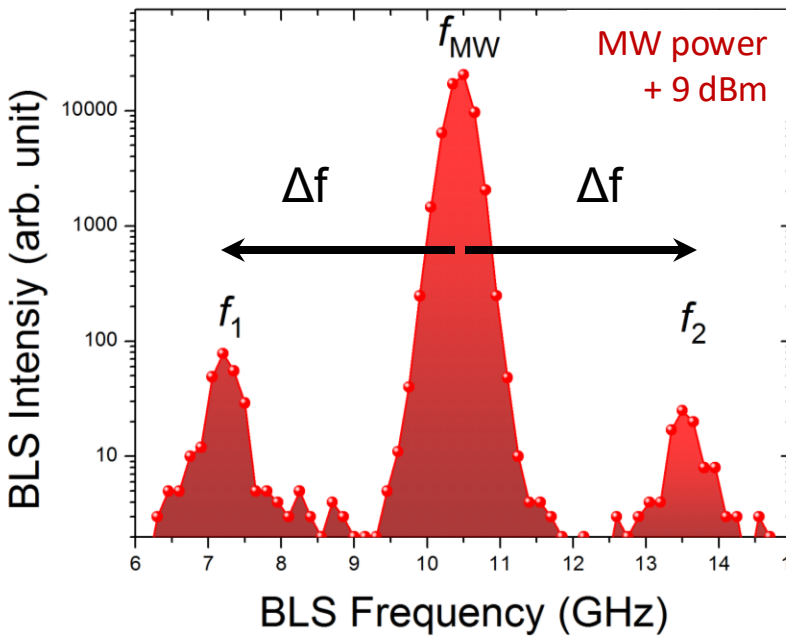


P. Pirro et al., Phys. Rev. Lett. **113**, 227601 (2014)

Four-magnon interactions in a spin-wave waveguide

Nonlinear regime

f_1, f_2 : unstable modes

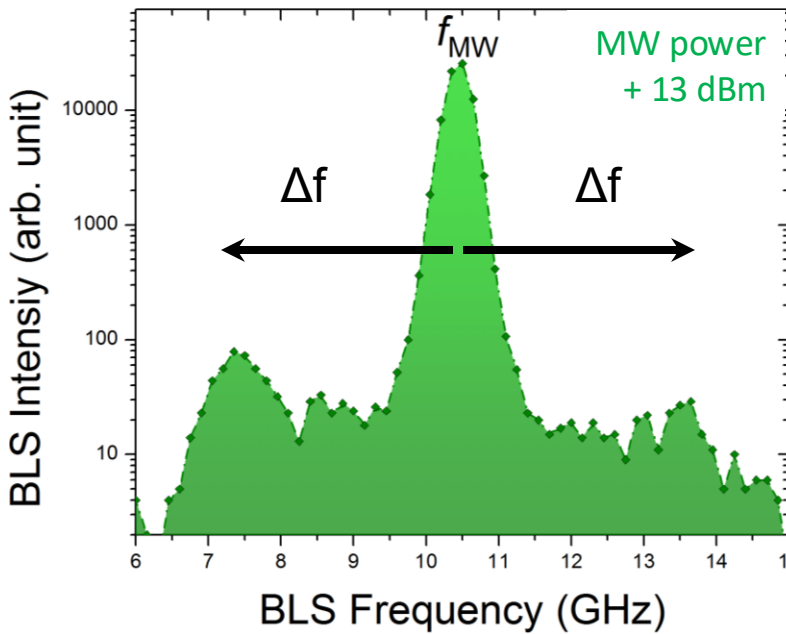


P. Pirro et al., Phys. Rev. Lett. **113**, 227601 (2014)

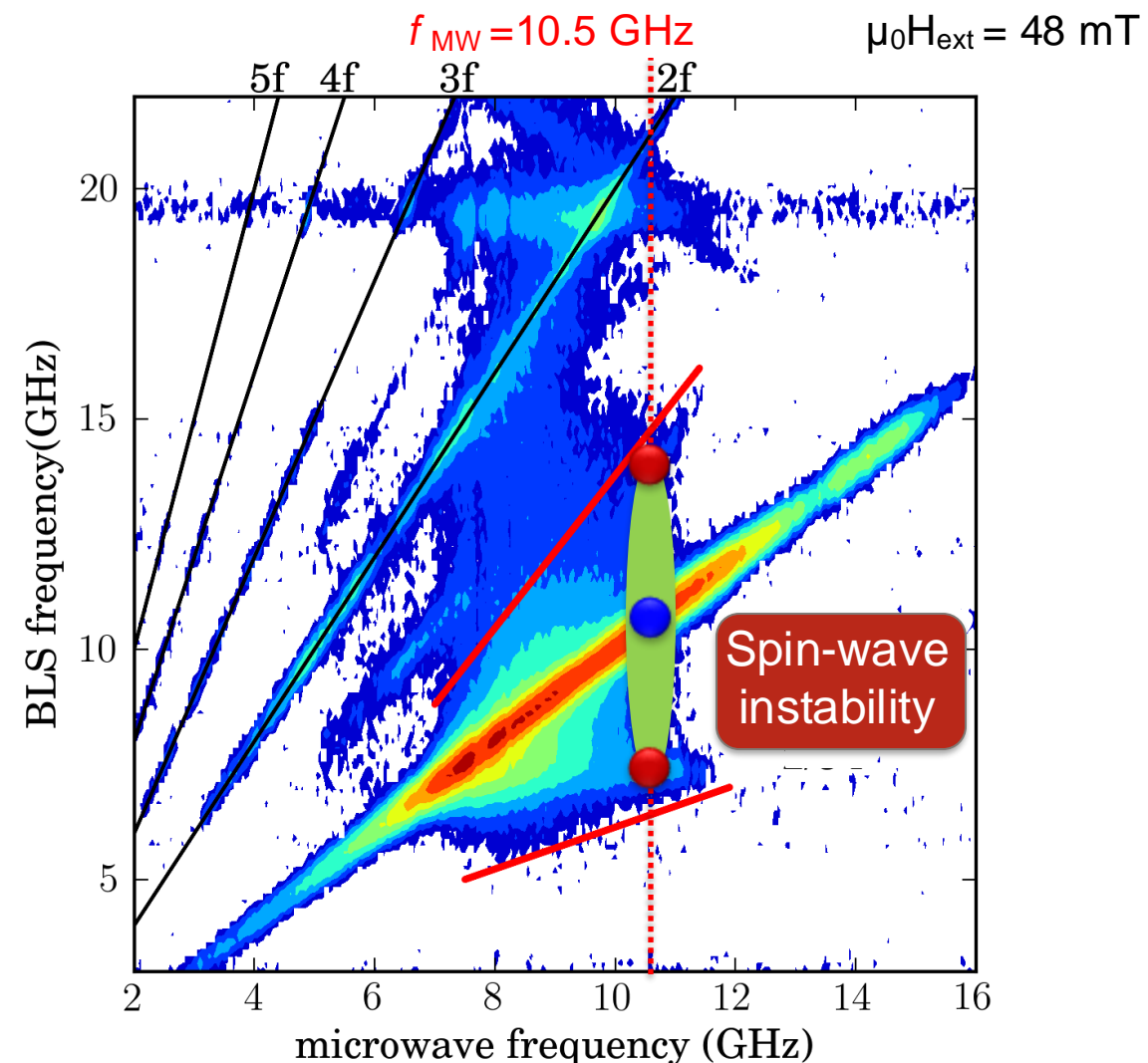
Four-magnon interactions in a spin-wave waveguide

Nonlinear regime

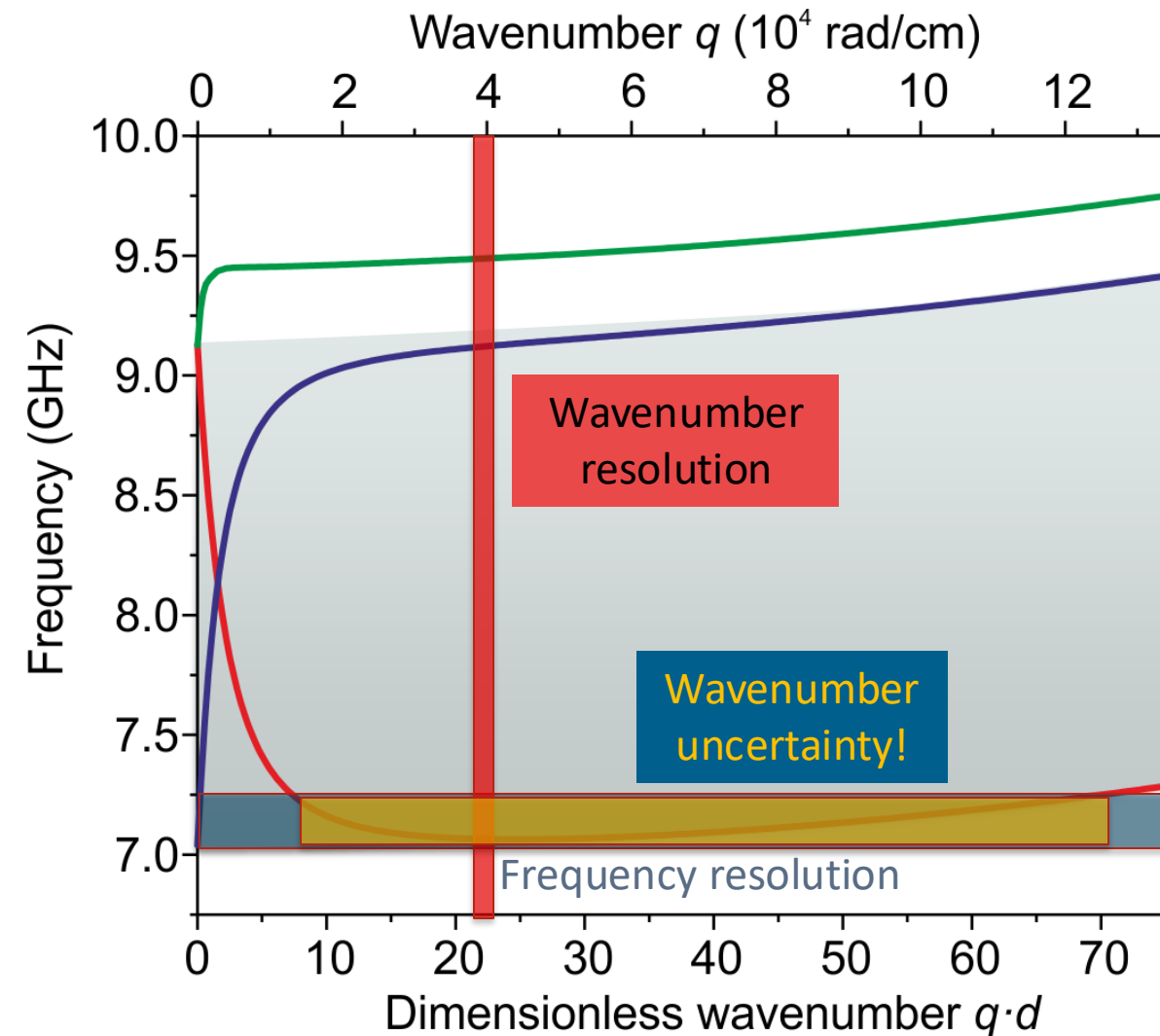
f_1, f_2 : unstable modes



P. Pirro *et al.*, Phys. Rev. Lett. **113**, 227601 (2014)

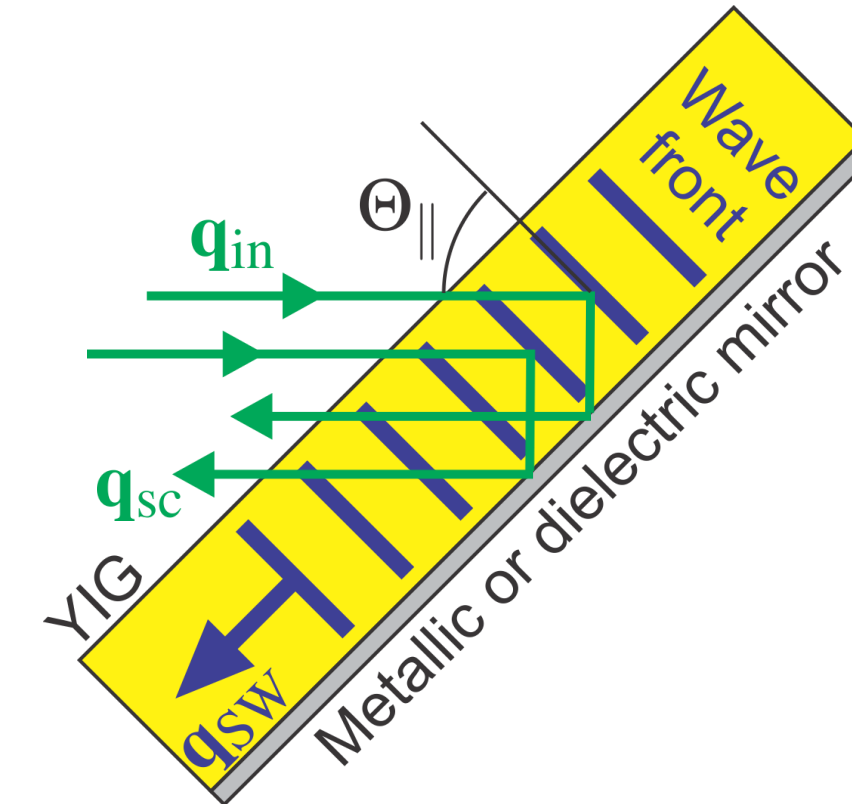
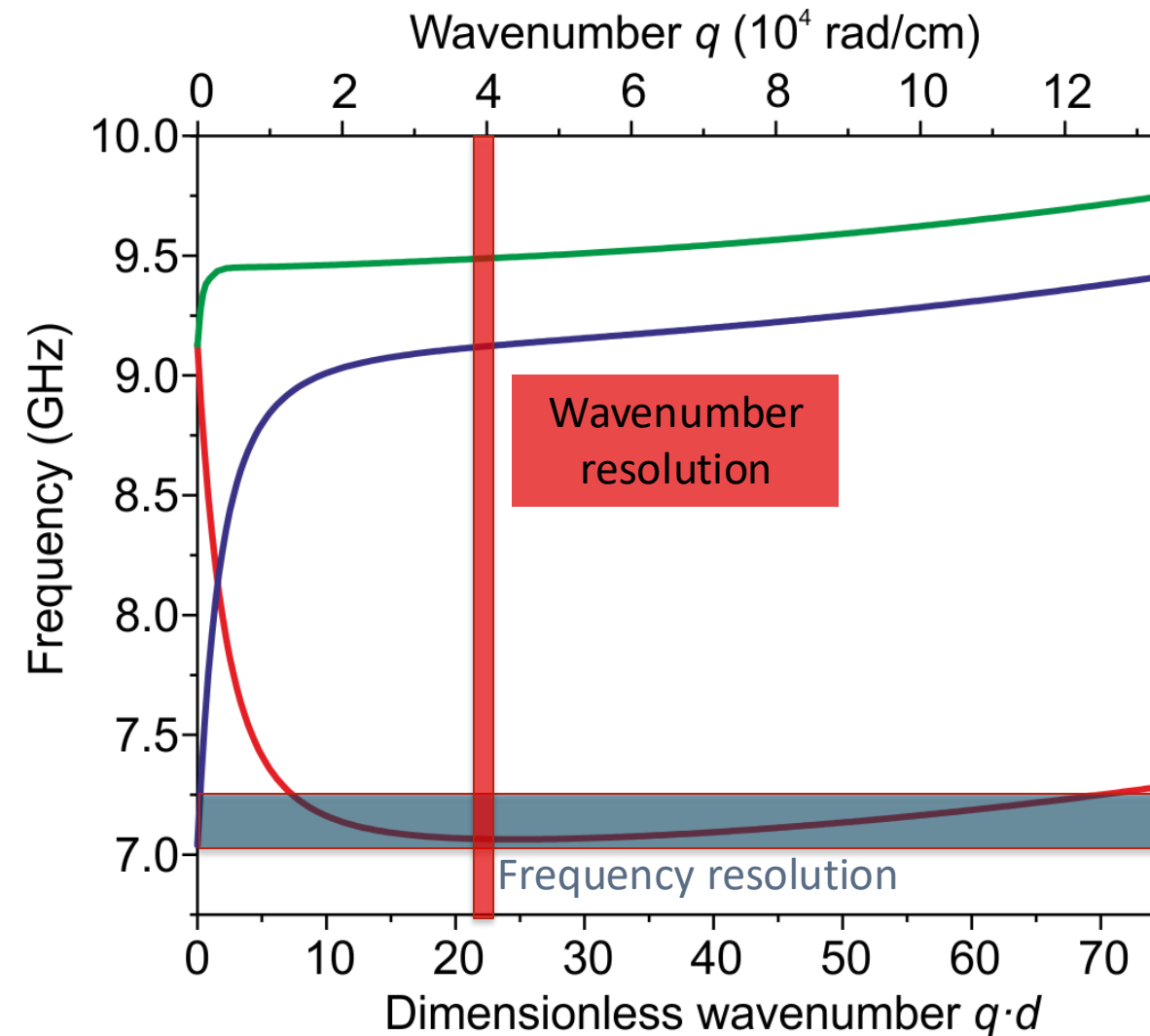


Wavenumber resolution principle



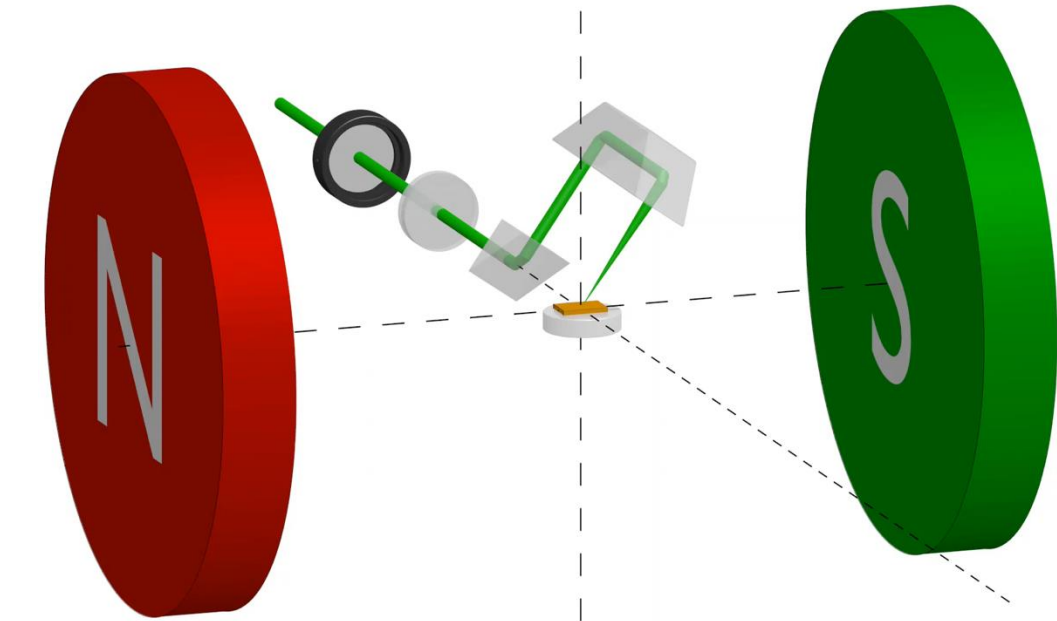
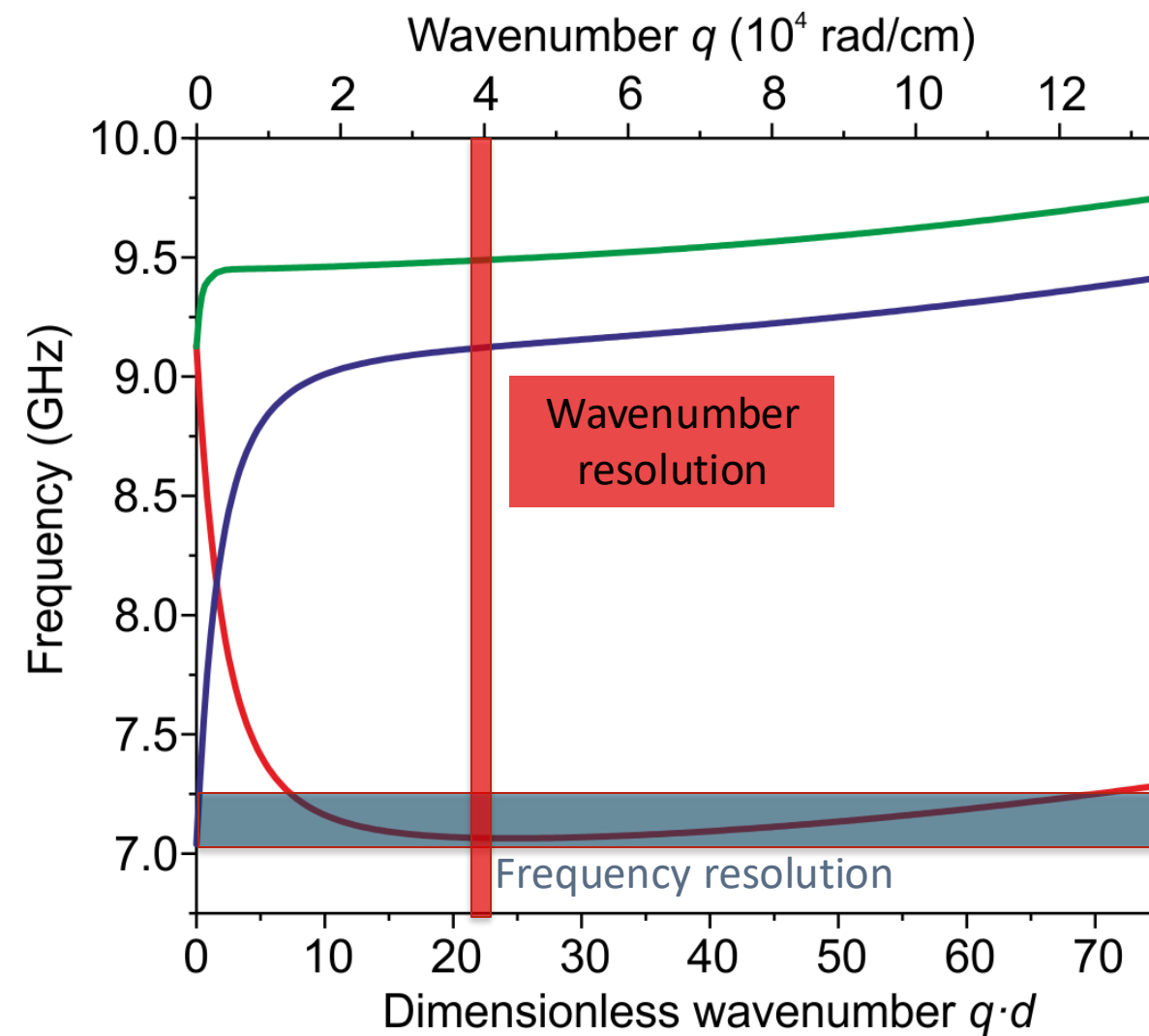
Wavenumber resolution principle

RP



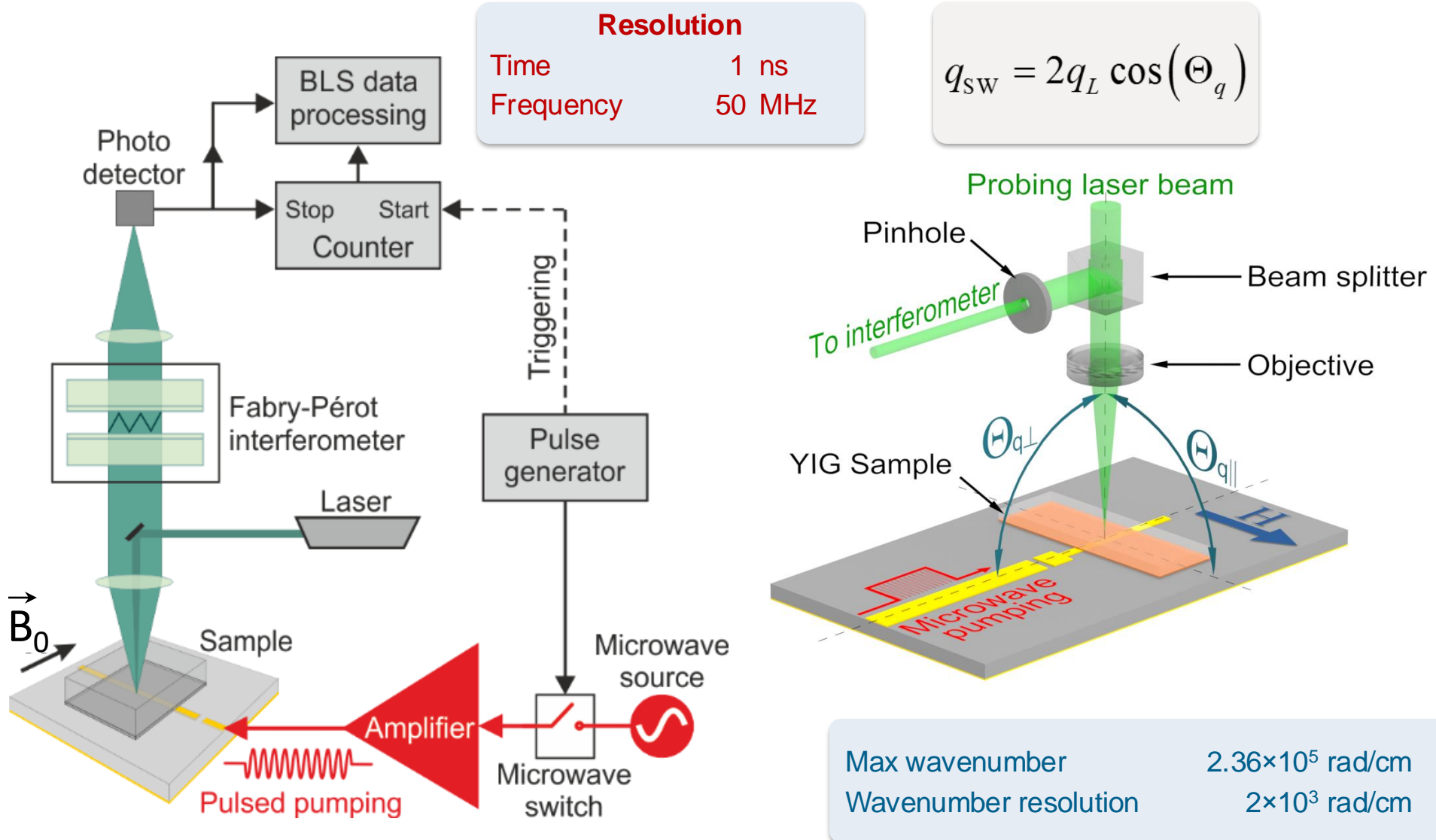
$$q_{\text{Spin wave}} = 2q_{\text{Laser}} \sin(\Theta_{\parallel})$$

Wavenumber resolution experiment



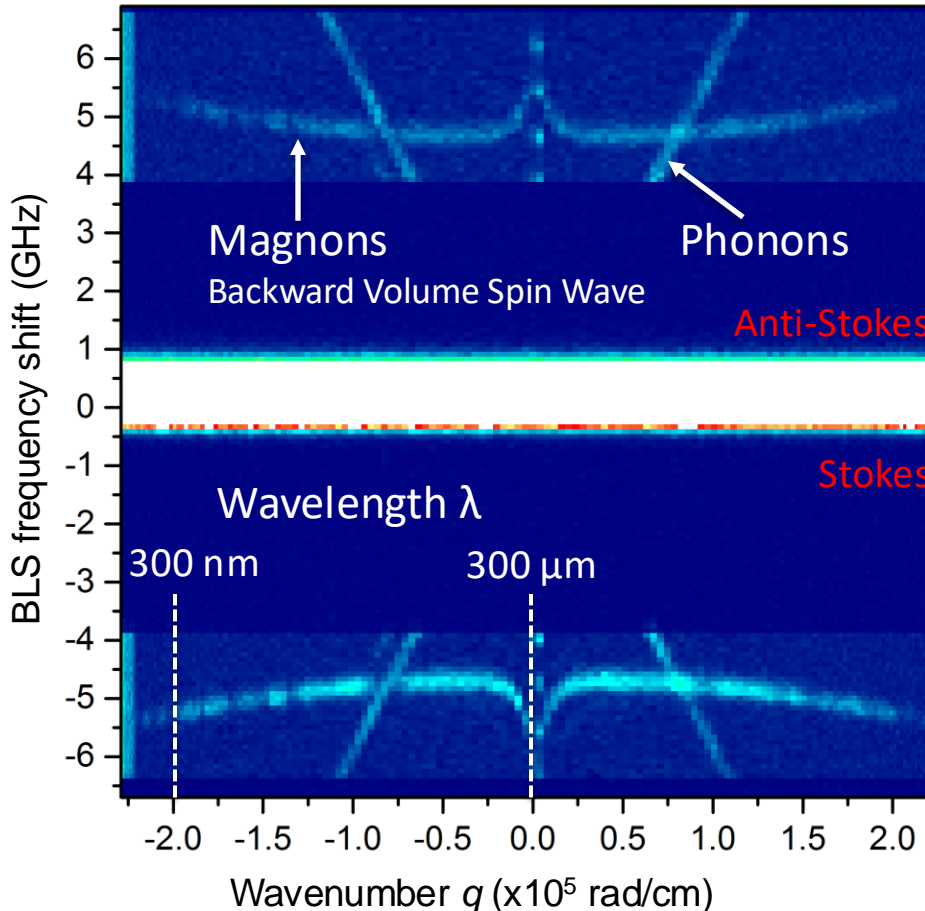
Max wavenumber 2.36×10^5 rad/cm
Wavenumber resolution 0.02×10^5 rad/cm

Time-, space- and wavevector-resolved Brillouin light scattering spectroscopy

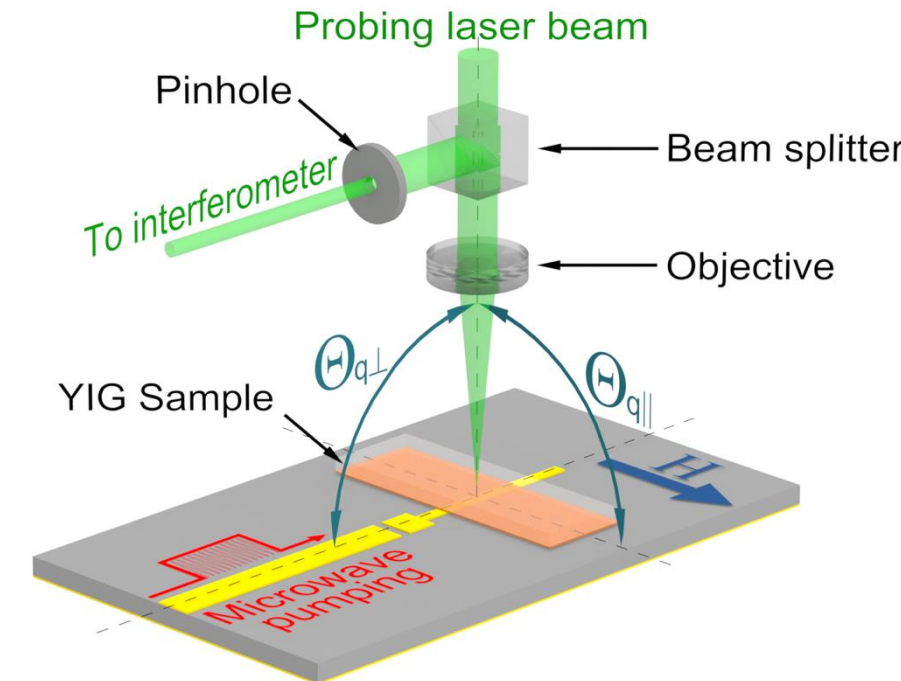


Wavevector-resolved BLS spectroscopy

Thermal spectrum of 6 μm thick YIG film



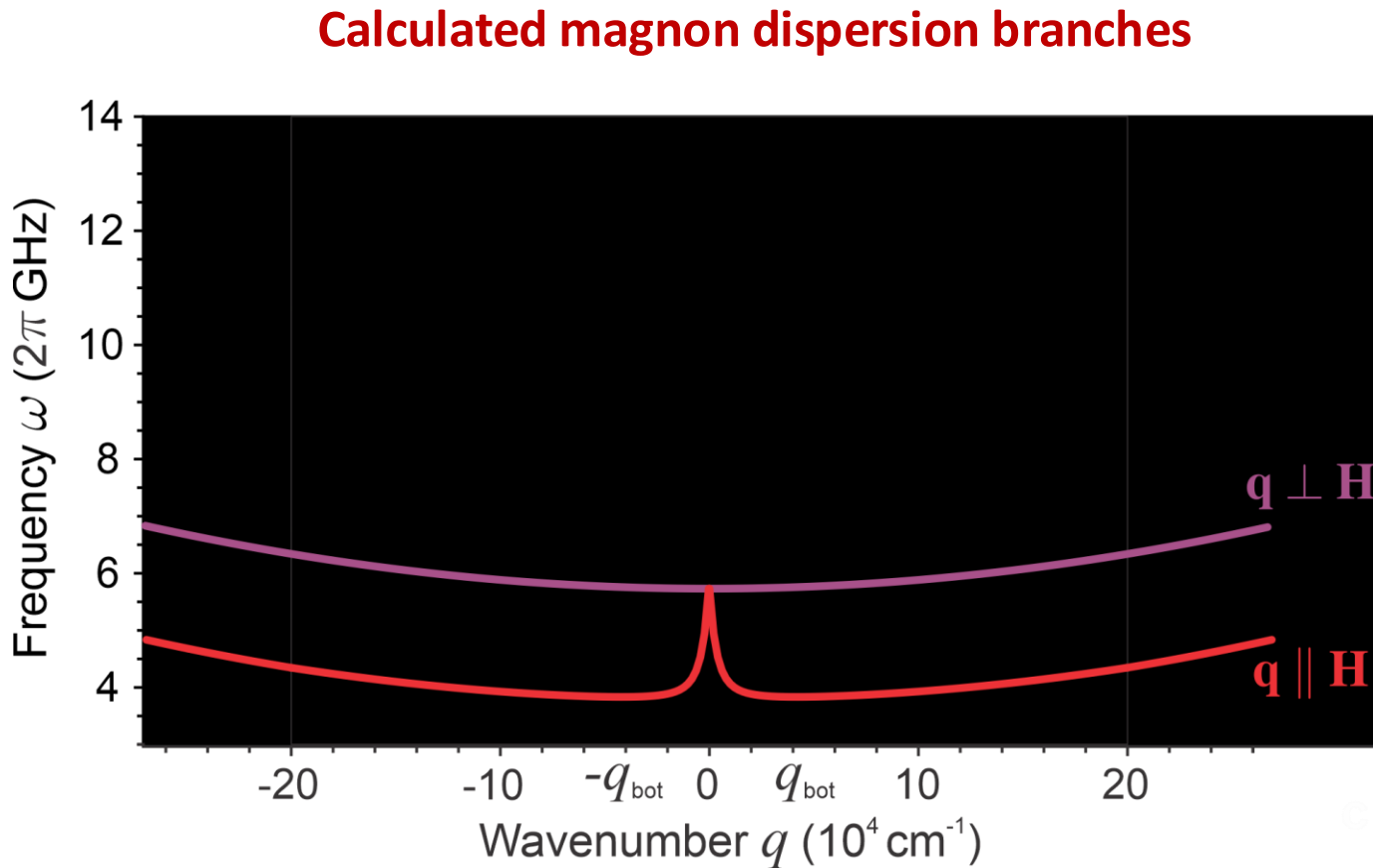
$$q_{\text{sw}} = 2q_L \cos(\Theta_q)$$



Max wavenumber
Wavenumber resolution

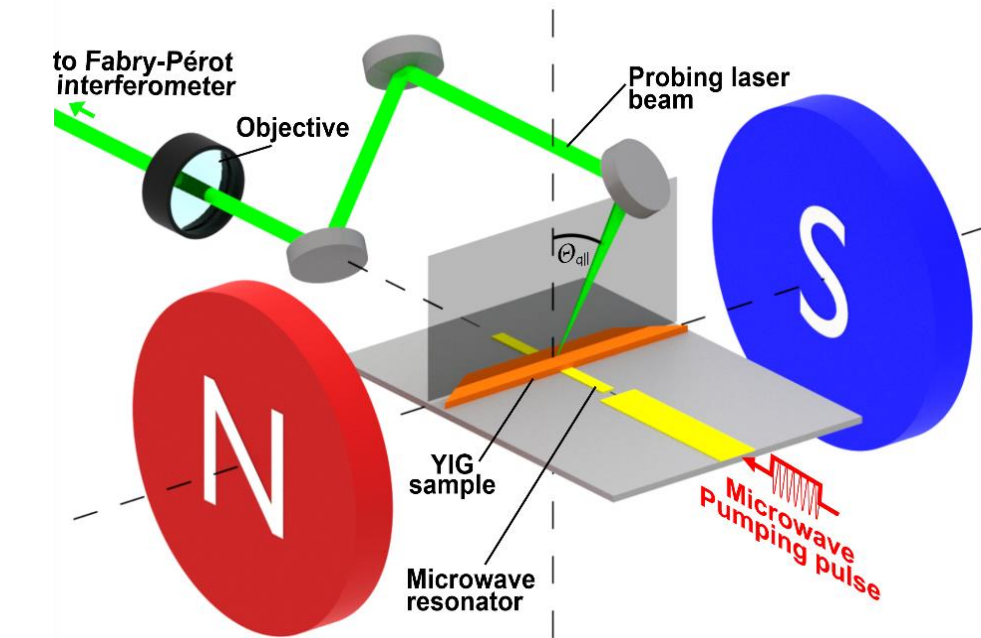
$2.36 \times 10^5 \text{ rad/cm}$
 $2 \times 10^3 \text{ rad/cm}$

Outlook: Pumped magnon spectra



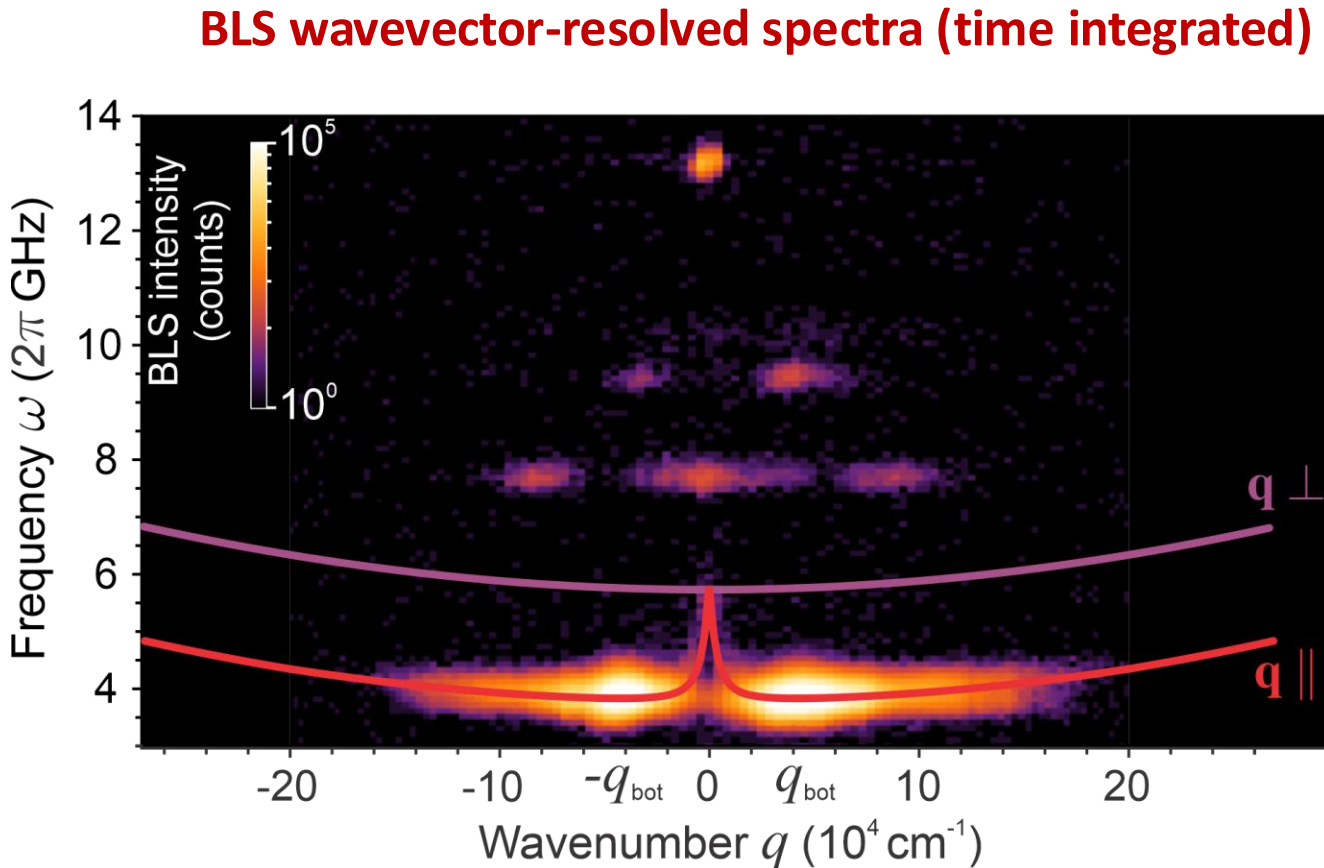
V. S. L'vov *et al.*, Phys. Rev. Lett. **131**, 156705 (2023)

BLS setup + microwave pumping circuit



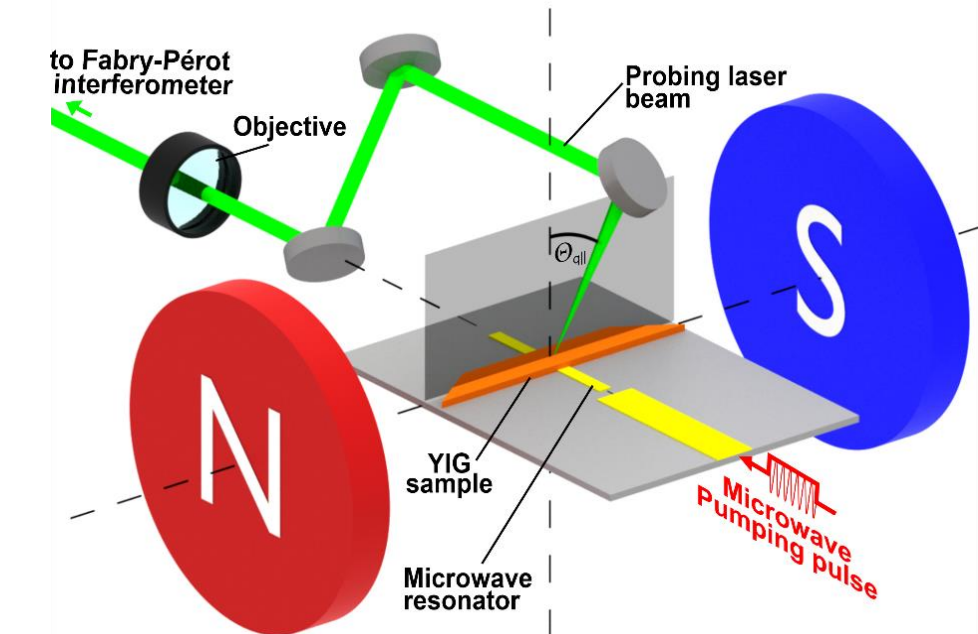
(111) LPE-grown YIG film:	6.7 μm
Width of the pumping area:	50 μm
Microwave power:	20 W
Pumping pulse:	1 μs
Pumping frequency:	13.2 GHz

Outlook: Pumped magnon spectra



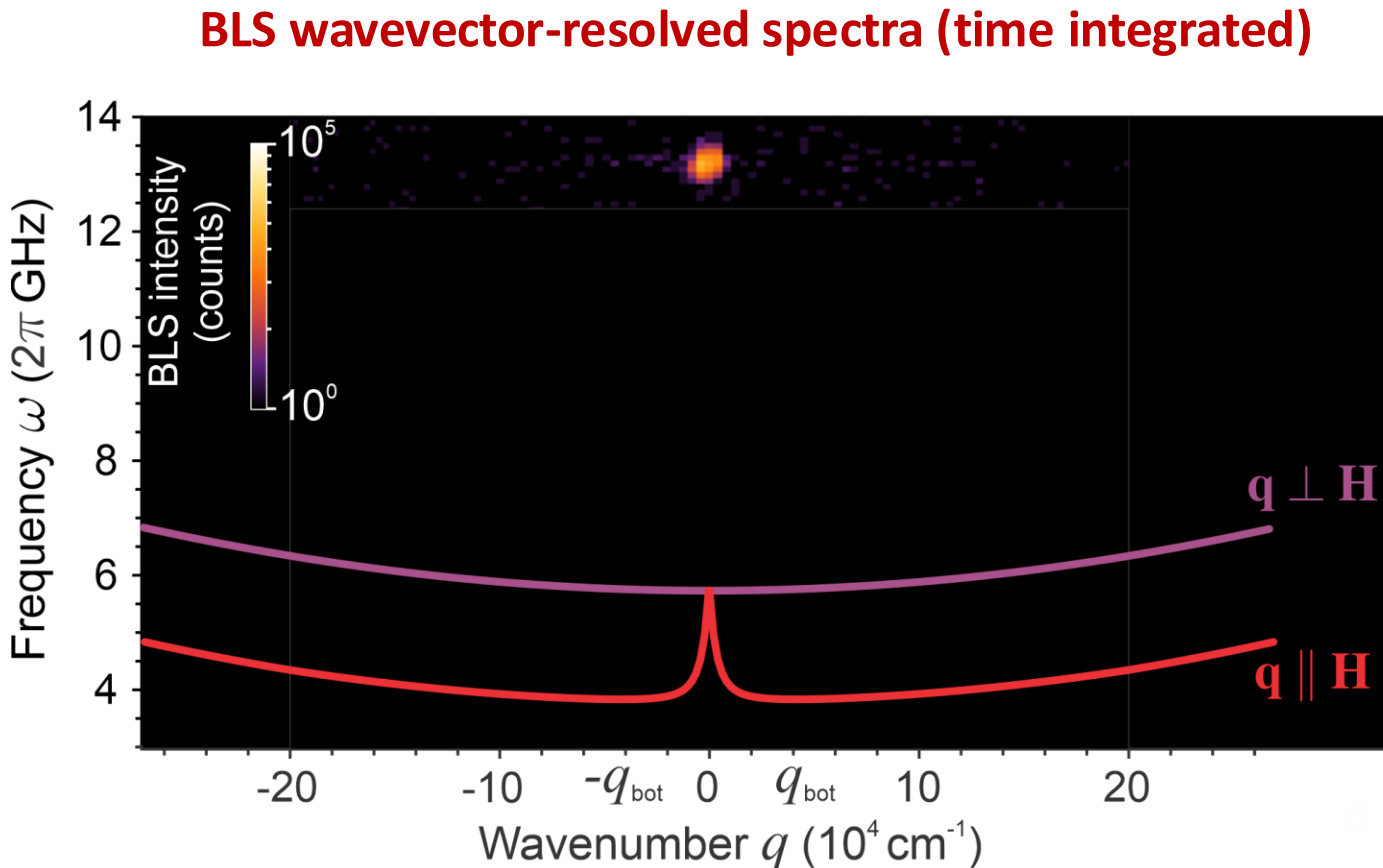
V. S. L'vov *et al.*, Phys. Rev. Lett. **131**, 156705 (2023)

BLS setup + microwave pumping circuit



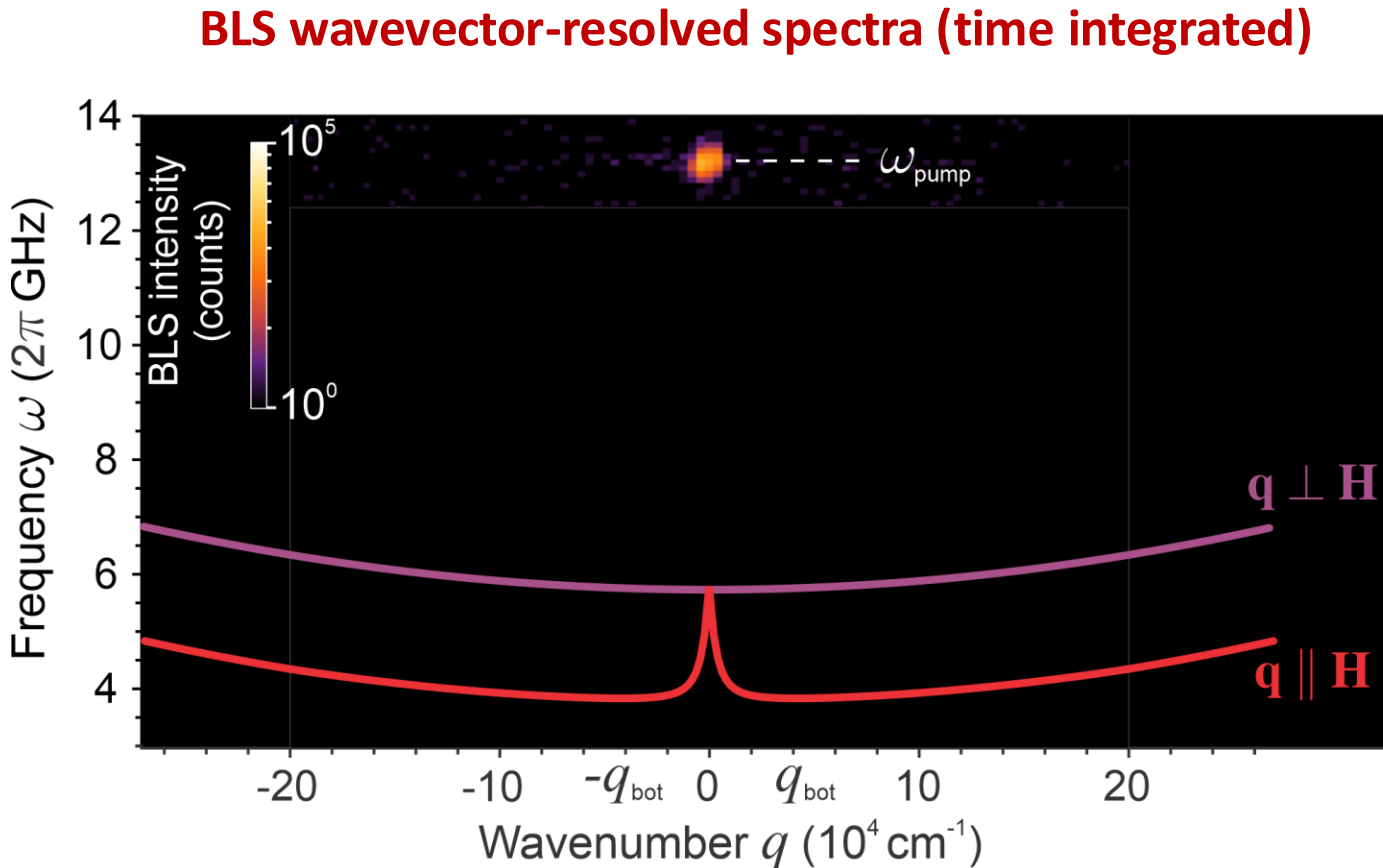
(111) LPE-grown YIG film:	$6.7 \mu\text{m}$
Width of the pumping area:	$50 \mu\text{m}$
Microwave power:	20 W
Pumping pulse:	$1 \mu\text{s}$
Pumping frequency:	13.2 GHz

Outlook: Pumped magnon spectra



V. S. L'vov *et al.*, Phys. Rev. Lett. **131**, 156705 (2023)

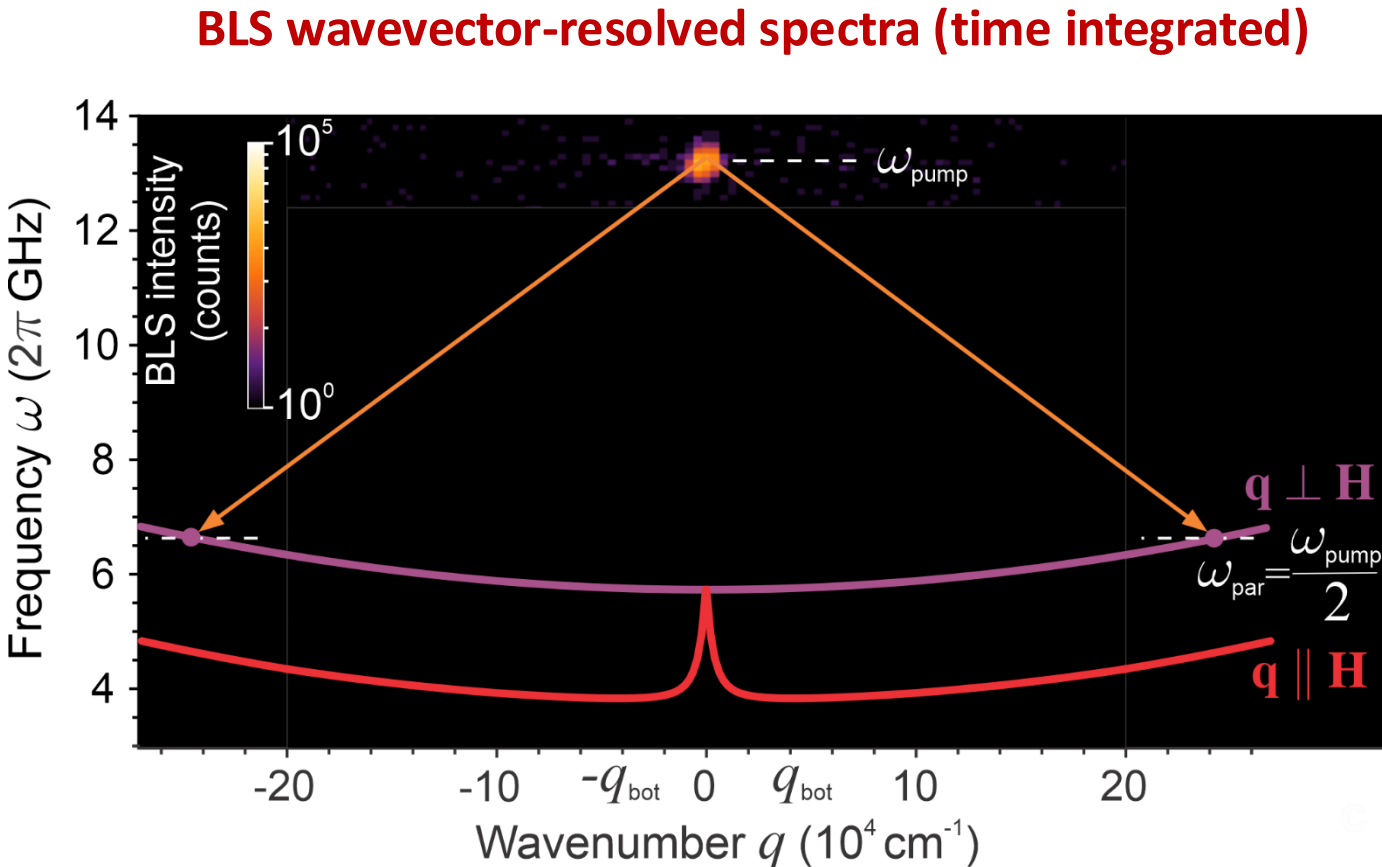
Outlook: Pumped magnon spectra



“Virtual” pumped,
forced magnons

V. S. L'vov *et al.*, Phys. Rev. Lett. **131**, 156705 (2023)

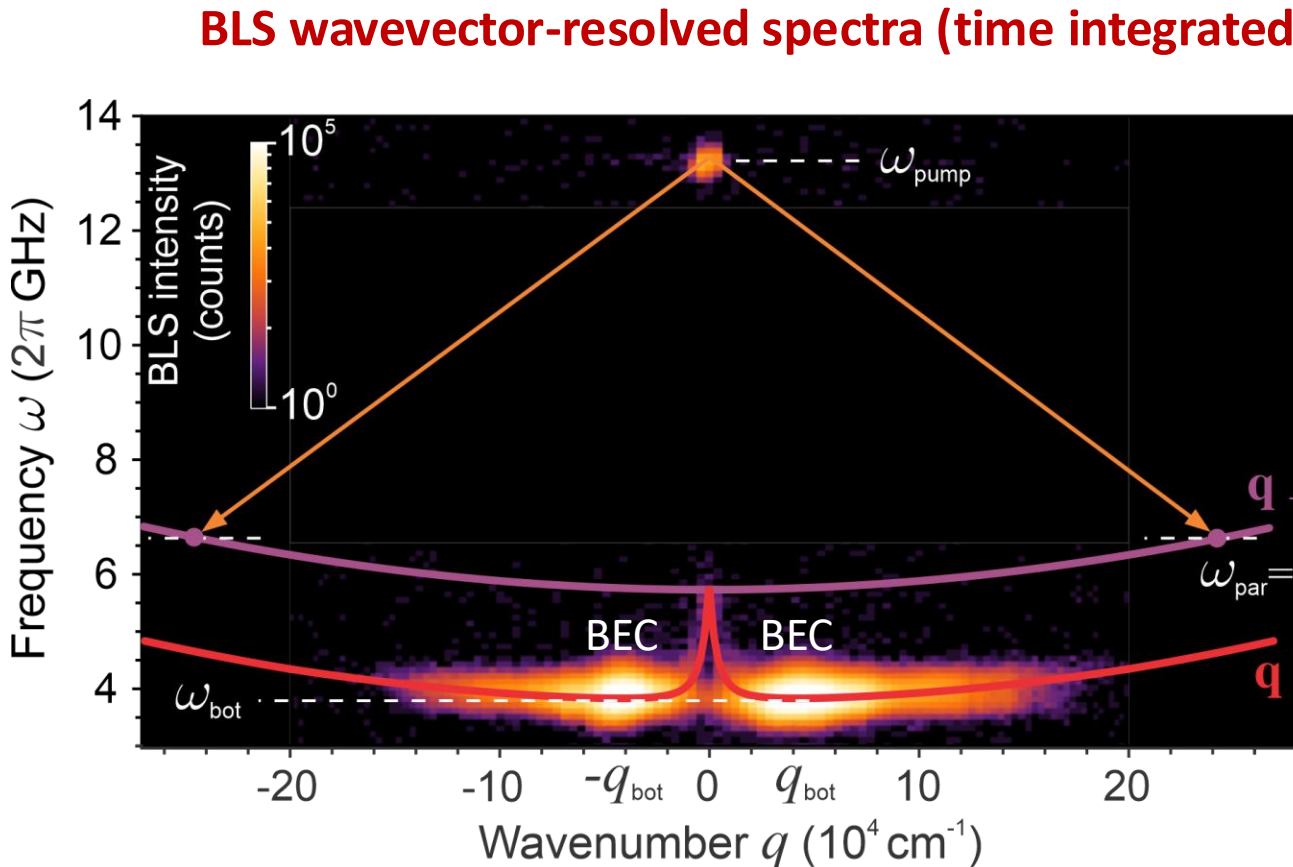
Outlook: Pumped magnon spectra



“Real” parametric magnons

V. S. L'vov *et al.*, Phys. Rev. Lett. **131**, 156705 (2023)

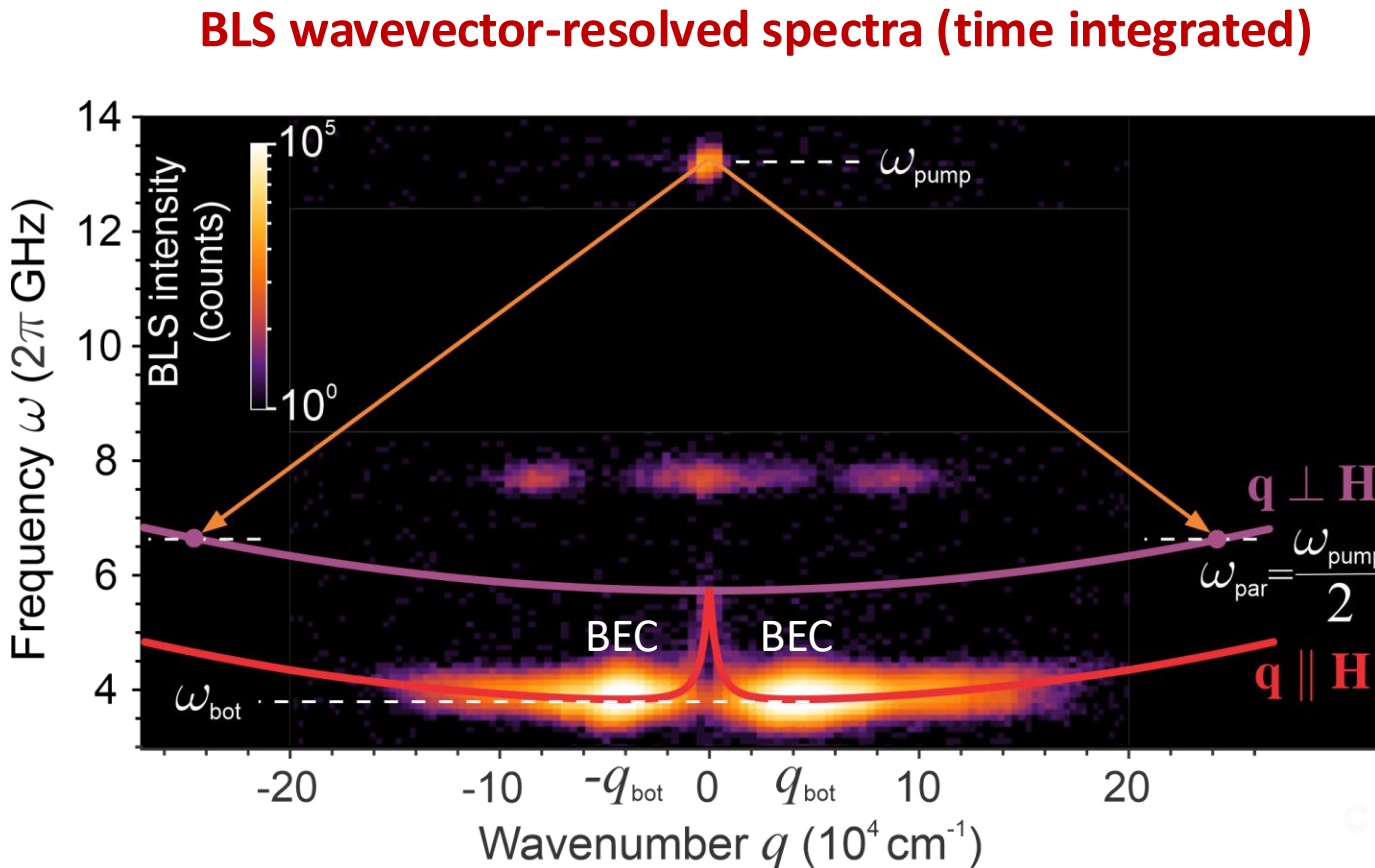
Outlook: Pumped magnon spectra



Magnon BEC
and magnon gas

V. S. L'vov *et al.*, Phys. Rev. Lett. **131**, 156705 (2023)

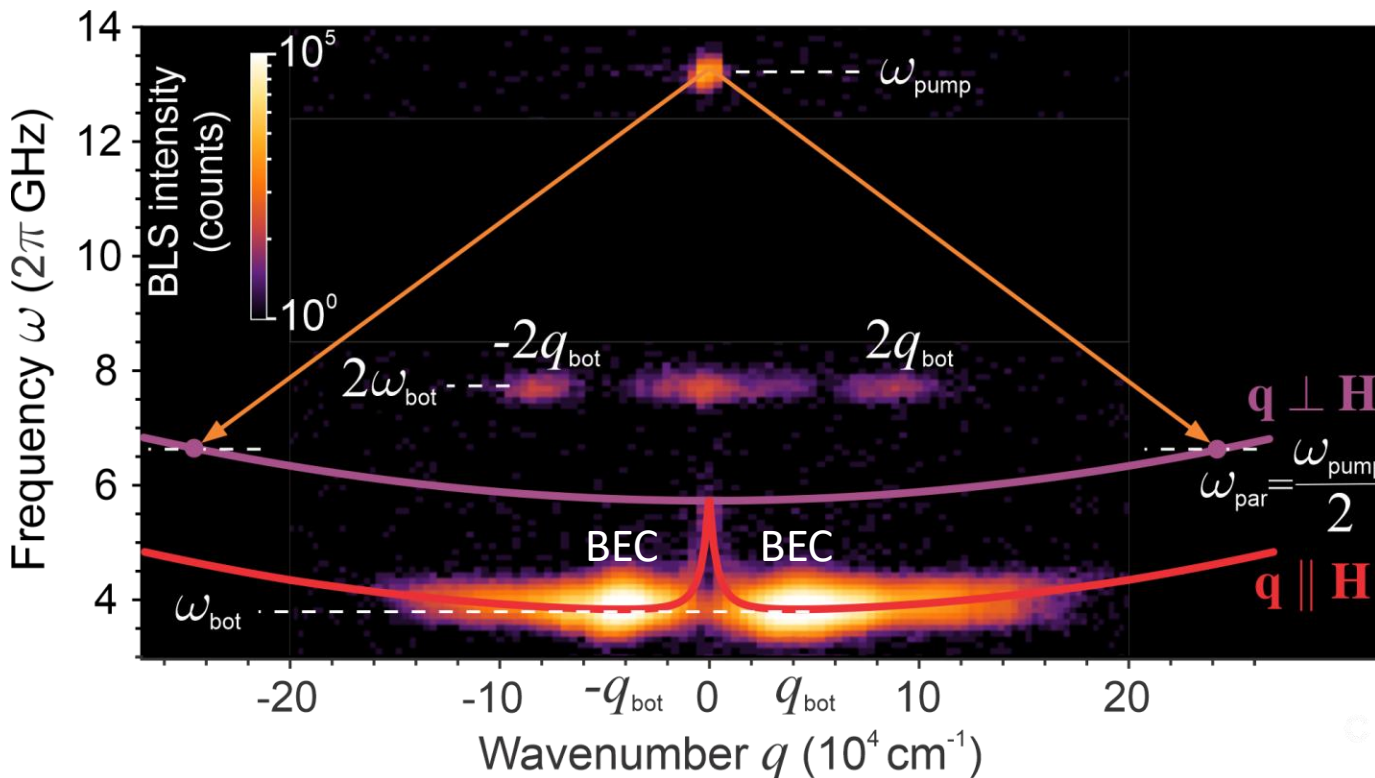
Outlook: Pumped magnon spectra



V. S. L'vov *et al.*, Phys. Rev. Lett. **131**, 156705 (2023)

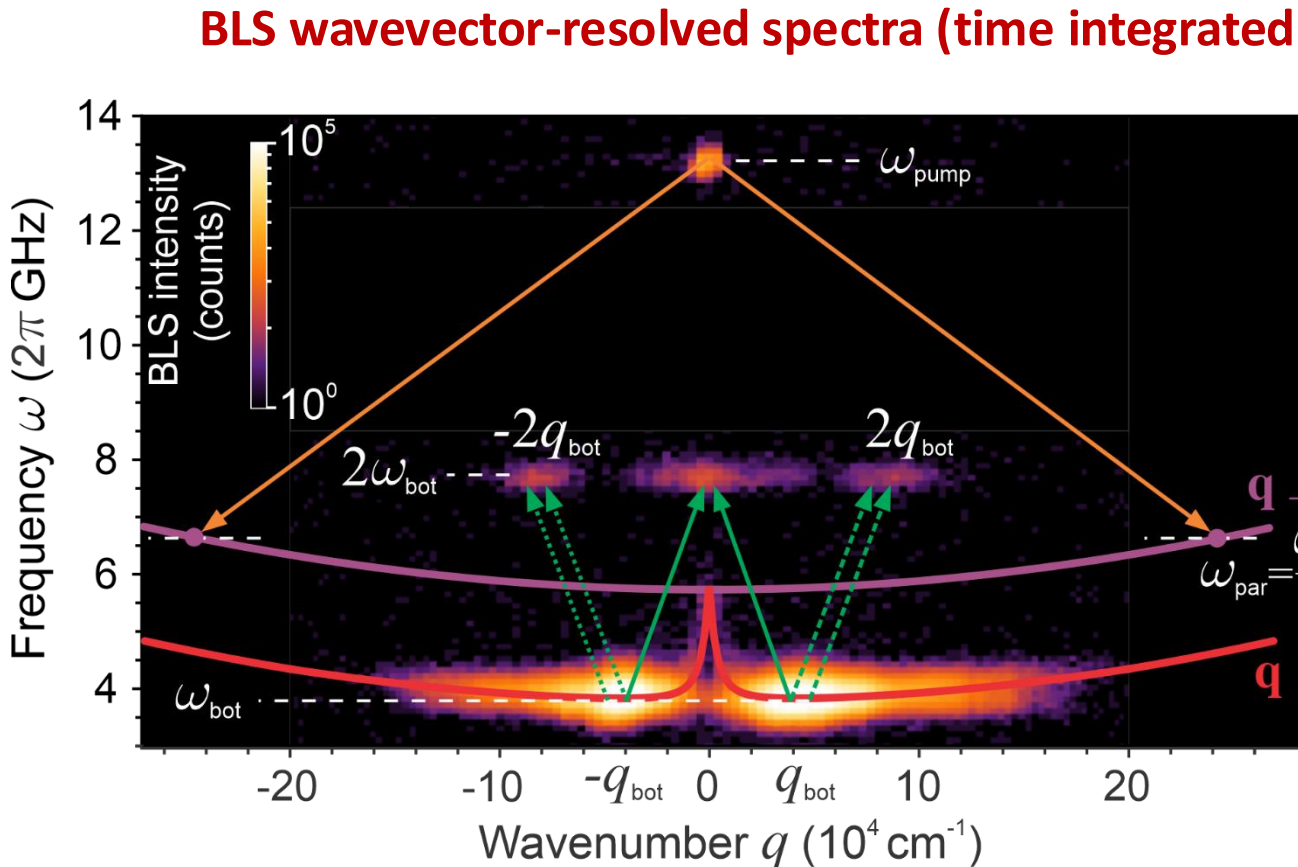
Outlook: Pumped magnon spectra

BLS wavevector-resolved spectra (time integrated)

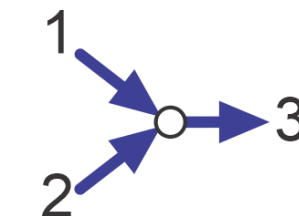


V. S. L'vov *et al.*, Phys. Rev. Lett. **131**, 156705 (2023)

Outlook: Pumped magnon spectra



Confluence processes:



Central spot:

$$\omega_{-q_{||}} + \omega_{+q_{||}} \Rightarrow 2\omega_{\text{bot}} \text{ and } q = 0$$

Left spot:

$$\omega_{-q_{||}} + \omega_{-q_{||}} \Rightarrow 2\omega_{\text{bot}} \text{ and } q = -2q_{\text{bot}}$$

Right spot:

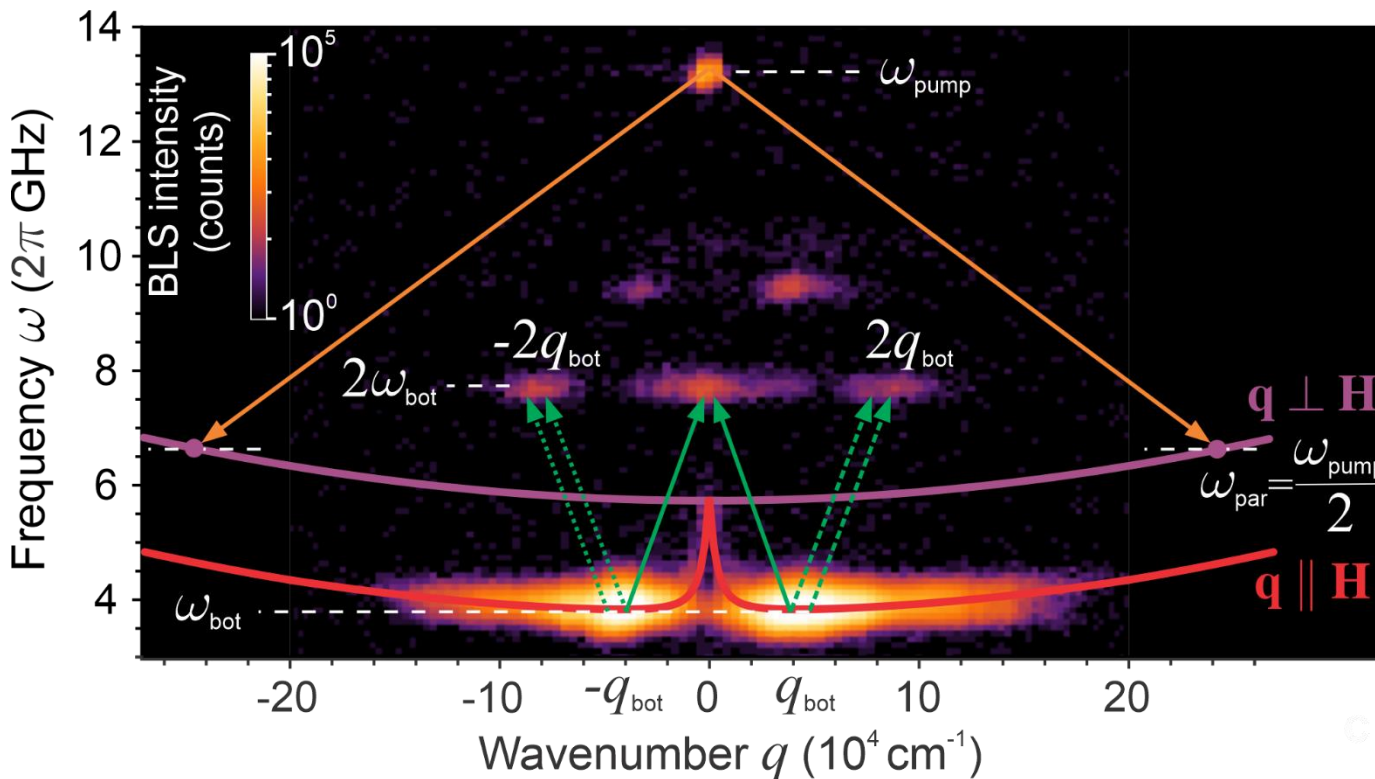
$$\omega_{+q_{||}} + \omega_{+q_{||}} \Rightarrow 2\omega_{\text{bot}} \text{ and } q = 2q_{\text{bot}}$$

“Double-bottom
virtual” magnons

V. S. L'vov *et al.*, Phys. Rev. Lett. **131**, 156705 (2023)

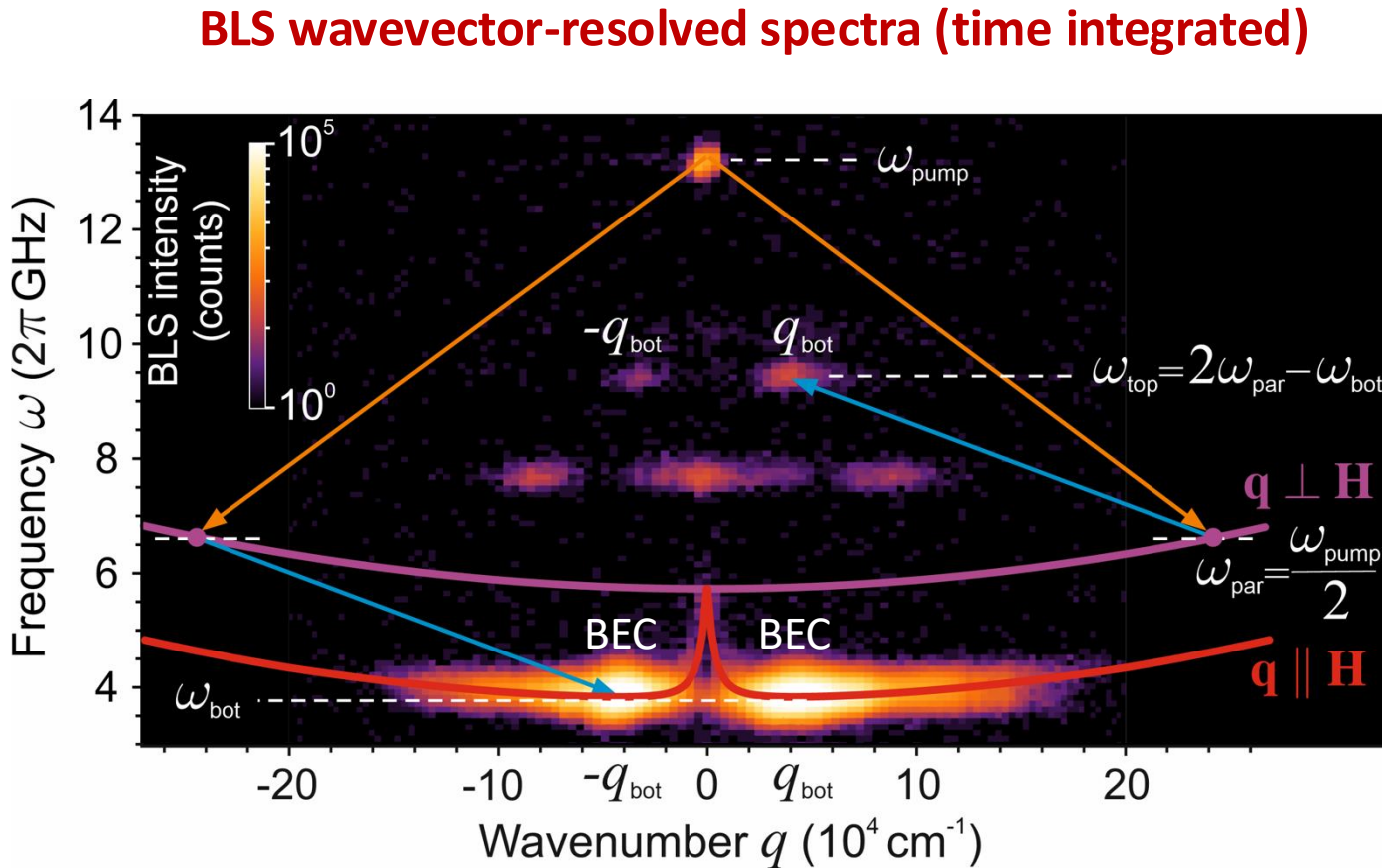
Outlook: Pumped magnon spectra

BLS wavevector-resolved spectra (time integrated)

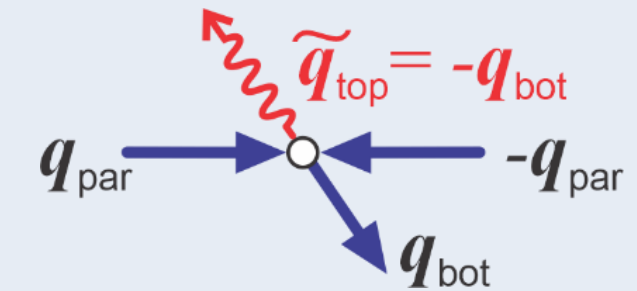


V. S. L'vov *et al.*, Phys. Rev. Lett. **131**, 156705 (2023)

Outlook: Pumped magnon spectra



4-magnon scattering process
similar to
the kinetic instability



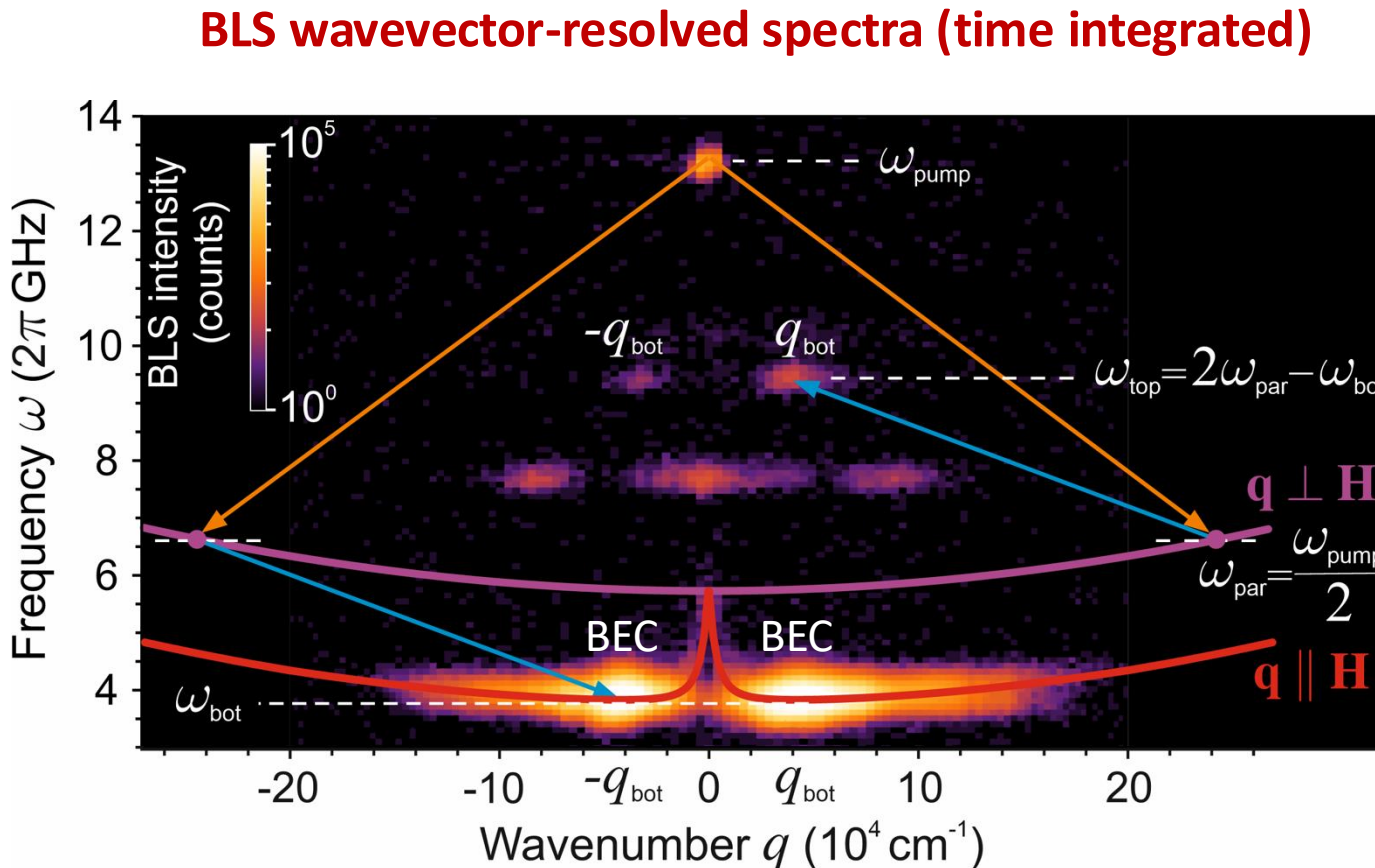
No magnon states with
 $(\omega_{\text{top}}, \pm q_{\text{bot}})$



negligibly weak process!

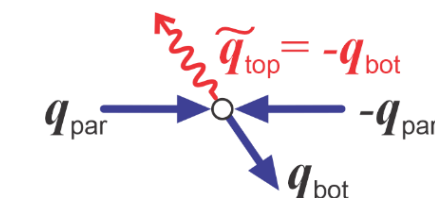
V. S. L'vov *et al.*, Phys. Rev. Lett. **131**, 156705 (2023)

Outlook: Pumped magnon spectra



- Full phase correlation in the pairs of parametric waves with $\pm q_{\text{par}}$
 - ↓
- Consider a pair of parametric magnons as a coherent wave object
 - ↓
- Therefore, such a four-magnon scattering process is **phase enhanced**

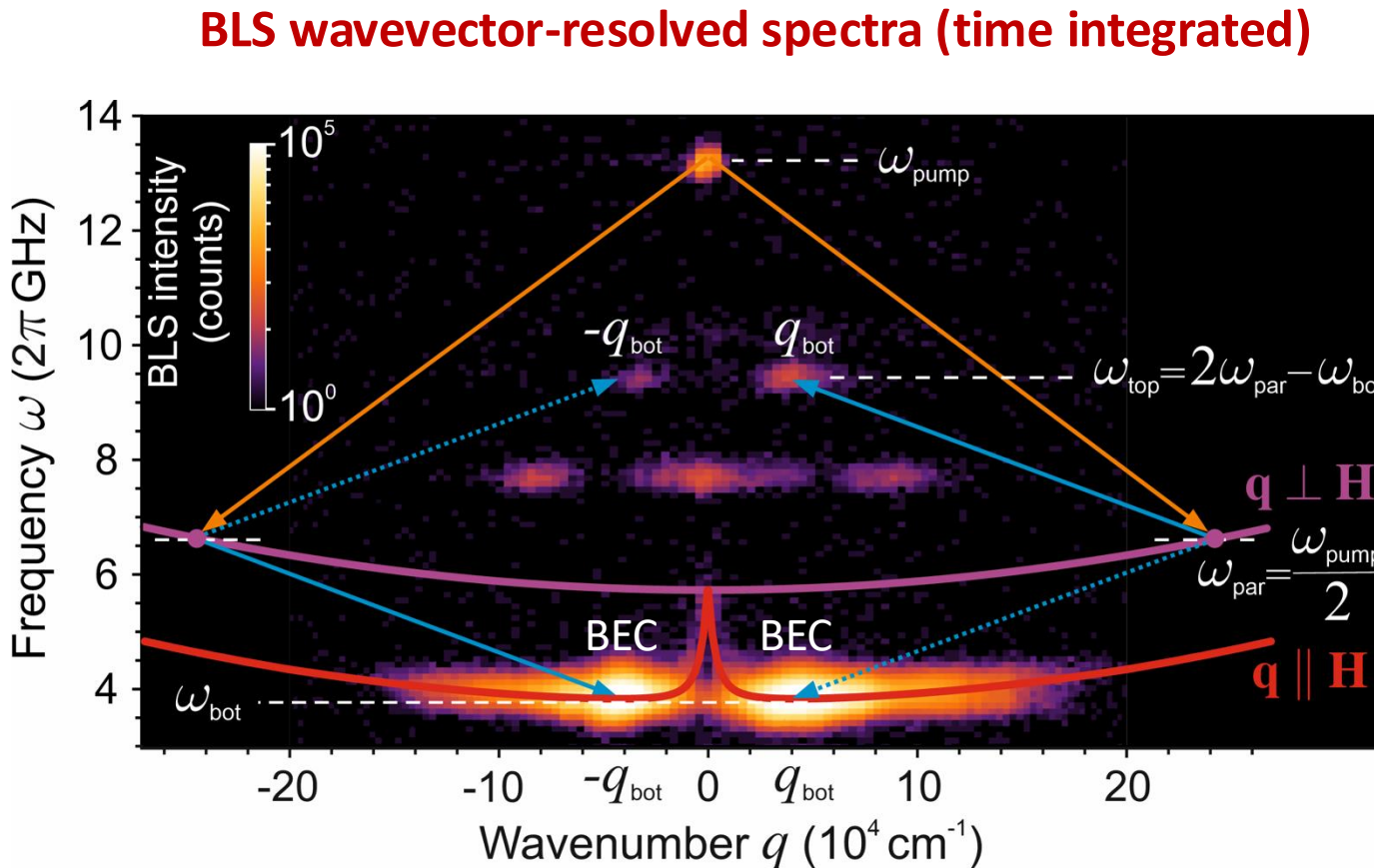
In quantum optics:
nonlinear processes with **quantum-correlated input** have higher efficiency



Classical version of
quantum enhancement

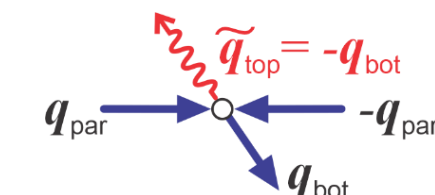
V. S. L'vov *et al.*, Phys. Rev. Lett. **131**, 156705 (2023)

Outlook: Pumped magnon spectra



- Full phase correlation in the pairs of parametric waves with $\pm q_{\text{par}}$
- Consider a pair of parametric magnons as a coherent wave object
- Therefore, such a four-magnon scattering process is **phase enhanced**

In quantum optics:
nonlinear processes with **quantum-correlated input** have higher efficiency



Classical version of
quantum enhancement

V. S. L'vov *et al.*, Phys. Rev. Lett. **131**, 156705 (2023)

Summary: What we leaned in this lecture:

- Ferromagnetic resonance and basics of microwave experiment with spin waves
- Brillouin light scattering (BLS) spectroscopy
- Time- and space-resolved BLS
- BLS microscopy
- Wavevector-resolved BLS
- Nonlinear processes
- Coherency might enlarge four-magnon processes – classical version of quantum enhancement